UNIVERSIDADE ESTADUAL PAULISTA – UNESP

Faculdade de Engenharia e Ciências - Campus de Guaratinguetá

JOÃO PEDRO RIBEIRO ROSA

HYBRID THERMODYNAMIC DEGRADATION MODEL FOR PROGNOSTICS OF PROTON EXCHANGE MEMBRANE FUEL CELL

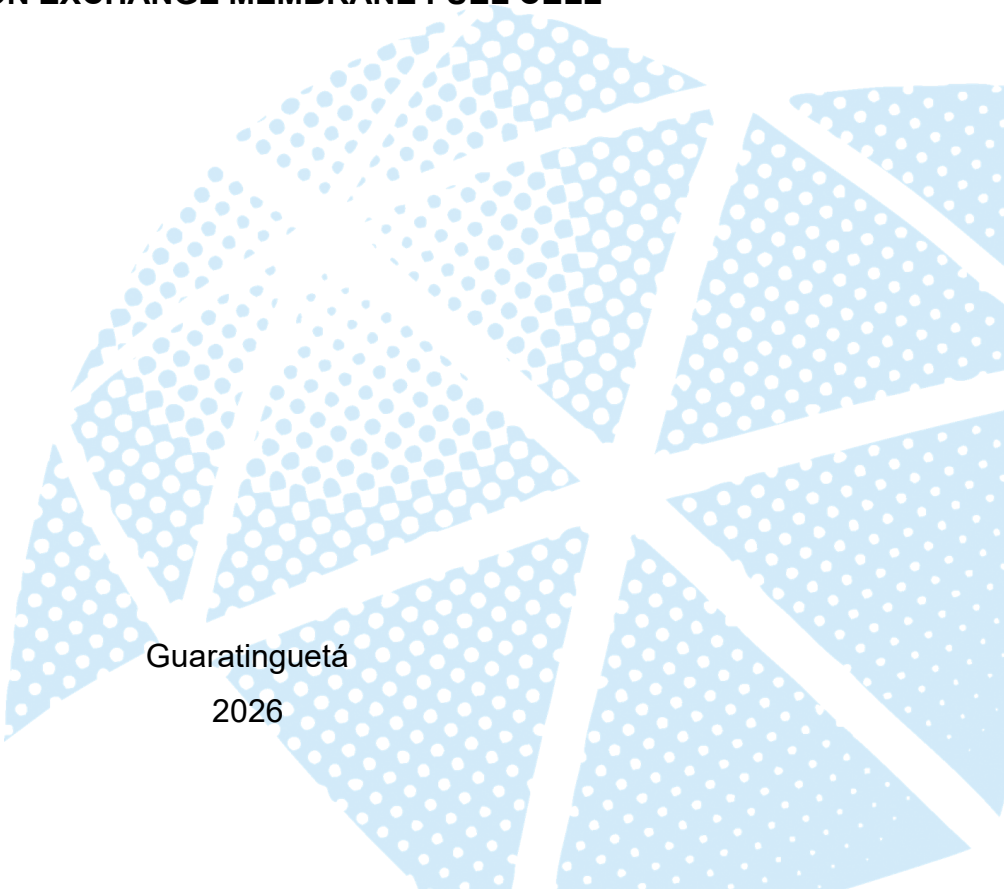

Guaratinguetá

2026

JOÃO PEDRO RIBEIRO ROSA

HYBRID THERMODYNAMIC DEGRADATION MODEL FOR PROGNOSTICS OF PROTON EXCHANGE MEMBRANE FUEL CELL

Dissertação apresentada à Universidade Estadual Paulista (UNESP), Faculdade de Engenharia e Ciências, Guaratinguetá, para obtenção do título de Grau acadêmico Mestre em Engenharia.

Área de Concentração: Mecânica

Orientador(a): Prof. Dr. José Alexandre Matelli

Coorientador(a): Dr. Chetan S. Kulkarni

Guaratinguetá

2026

Rosa, João Pedro Ribeiro
R788h Hybrid thermodynamic degradation model for prognostics of proton exchange membrane fuel cell / João Pedro Ribeiro Rosa - Guaratinguetá, 2026.
59 f : il.
Bibliografia: f. 47-52

Dissertação (Mestrado) – Universidade Estadual Paulista, Faculdade de Engenharia e Ciências de Guaratinguetá, 2026.

Orientador: Prof. Dr. José Alexandre Matelli
Coorientador: Prof. Dr. Chetan S. Kulkarni

1. Células à combustível. 2. Termodinâmica. 3. Física estatística. 4. Eletroquímica. I. Título.

CDU 662.7(043)

Luciana Máximo
Bibliotecária/CRB-8 3595

POTENTIAL IMPACT OF THIS RESEARCH

This master's research project proposed a new prognostics method of evaluating the remaining useful life of proton exchange membrane fuel cells and its energy exchange efficiency during its lifetime. Currently, fuel cells have limited usage due to its short lifetime and high costs. On the other hand, fossil fuels, the main cause of greenhouse effects, are burned more and more to sustain the increasing energy demand. Building on this foundation, we believe that the main societal impact that this work could generate is a more reliable usage of proton exchange fuel cells as a clean energy source.

JOÃO PEDRO RIBEIRO ROSA

HYBRID THERMODYNAMIC DEGRADATION MODEL FOR PROGNOSTICS OF PROTON EXCHANGE MEMBRANE FUEL CELL.

Dissertação apresentada à Universidade Estadual Paulista (UNESP), Faculdade de Engenharia e Ciências de Guaratinguetá, para obtenção do título de Mestre em Engenharia

Data da defesa: 17/03/2026

Banca Examinadora:

gov.br
Documento assinado digitalmente
JOSE ALEXANDRE MATELLI
Data: 08/04/2026 08:17:41-0300
Verifique em https://validar.iti.gov.br

Prof. Dr. JOSÉ ALEXANDRE MATELLI

Orientador - UNESP

gov.br
Documento assinado digitalmente
EDUARDO GONCALVES CIAPINA
Data: 04/05/2026 08:37:04-0300
Verifique em https://validar.iti.gov.br

Prof. Dr. EDUARDO GONÇALVES CIAPINA

UNESP

ICP-Edu
Documento assinado digitalmente
Amir Antonio Martins de Oliveira Junior
Data: 08/04/2026 12:22:59-0300
CPF: ***.526.889-**
Verifique as assinaturas em https://v.ufsc.br

Prof. Dr. AMIR ANTÔNIO MARTINS OLIVEIRA JÚNIOR

UFSC

ACKNOLEDGEMENTS

I would like to express my gratitude to everyone that helped during this graduate course.

To my advisors Prof. José Alexandre Matelli and Dr. Chetan Kulkarni, who have helped every step of the way, providing help and orientations not only for the project but also to the endless documents.

To the friends of NASA Ames Research Center, especially the folks of Diagnostics and Prognostics Group, for welcoming me during my stay and the sharing of knowledge and experiences.

To the librarians and my professors at São Paulo State University, for answering my endless questions.

To Coordenação de Aperfeiçoamento de Pessoal de Nível Superior – Brasil (CAPES) – Finance code 001, for the fincancial support.

To São Paulo State Research Foundation (FAPESP), for the financial support, granted through process number 2024/00161-9 and 2025/02847-8.

And finally, I would like to thank my parents, Cláudio Henrique Rosa and Patrícia Monteiro Ribeiro, and my brother, Gabriel Ribeiro Rosa, for all the love and support.

ABSTRACT

In the context of increased energy demand and increased problems due to carbon emissions, fuel cells emerge as a promising solution. However, its low durability and high cost still prevent its commercialization on a large scale. Degradation of fuel cell performance can be caused by several reasons, such as thermal and mechanical stress, humidity conditions, variable load profiles and start/stop conditions. Still, this phenomenon is not fully understood. To extend fuel cell lifetime, prognostics and health management (PHM) are gaining attention. The prognosis aims to estimate the remaining useful life of the system (RUL) and degradation trends to assist in performing predictive maintenance. There are two main approaches to prognosis: data-driven methods and model-based methods. While data-driven methods may be more accurate in estimating RUL and are easier to implement, they suffer from overfitting issues and require specialized knowledge to fit state-of-the-art models. Model-based methods on the other hand lack accuracy and ease of being applied. Thus, this masters project proposed a hybrid-based prognostic method obtained through a fuel cell entropy generation analysis. The proposed method was able to accurately advance entropy generations states of the cell through time and predict long-term polarization curve decay. It was further shown that entropy generation metric could be used to define an easier to be predicted end of life criteria, useful to maintenance procedures scheduling.

Keywords: Prognosis; fuel cell; degradation; thermodynamic model.

RESUMO

No contexto do aumento da demanda energética e aumento dos problemas devido às emissões de carbono, as células de combustível surgem como uma solução promissora. No entanto, sua baixa durabilidade e alto custo ainda impedem sua comercialização em larga escala. A degradação do desempenho da célula de combustível pode ser causada por várias razões, como estresse térmico e mecânico, condições de umidade, perfis de carga variáveis e condições de partida/parada. Ainda assim, esse fenômeno não é totalmente compreendido. Para prolongar a vida útil das células de combustível, prognósticos e manutenção da vida útil (PHM) estão ganhando atenção. O prognóstico visa estimar a vida útil restante do sistema (RUL) e as tendências de degradação para auxiliar na realização da manutenção preditiva. Existem duas abordagens principais para o prognóstico: métodos orientados por dados e métodos baseados em modelos. Embora métodos orientados por dados possam ser mais precisos na estimativa da RUL e mais fáceis de serem implementados, eles sofrem de problemas de sobre ajuste e exigem conhecimento especializado para adaptar os modelos estado-da-arte. Métodos baseados em modelos, por outro lado, carecem de precisão e facilidade de aplicação. Assim, este projeto de mestrado propôs um método prognóstico híbrido obtido por meio de uma análise de geração de entropia da célula de combustível. O método proposto foi capaz de avançar com precisão os estados de geração de entropia da célula ao longo do tempo e prever o decaimento da curva de polarização a longo prazo. Foi ainda demonstrado que a métrica de geração de entropia poderia ser usada para definir critérios de fim de vida mais fáceis de serem previstos, úteis para o agendamento de procedimentos de manutenção.

Palavras-chave: Prognóstico; célula de combustível; degradação; modelo termodinâmico.

LIST OF FIGURES

LIST OF TABLES

SUMMARY

1 INTRODUCTION

In the context of increasing energy demand and problems due to carbon emissions, fuel cells appear as a promising solution in an energy transition scenario (Petrone et al., 2013). The fuel cell is an electrochemical device that converts chemical energy directly into electrical energy. Each unit cell consists mainly of a positive electrode (cathode), a negative electrode (anode), and an electrolyte (Barbir, 2012). Fuel cells are classified according to their electrolytes and fuels used (Lucia, 2014; Shah, 2007). In this work, a proton exchange membrane fuel cell (PEMFC) is the object of study.

The structure of a PEMFC unit cell is illustrated in Figure 1. Hydrogen gas is supplied to the anode, where it flows through the gas diffusion layer and oxidizes in the catalyst layer. Hydrogen ions flow through the polymeric membrane and electrons are conducted through the external circuit, generating an electric current. Hydrogen ions and electrons meet in the catalyst layer of the cathode along with oxygen to generate water (Litster; McLean, 2004). As each cell provides about 1 V, the voltage can be increased by arranging cells in series (the cells are then said to be stacked). The output voltage depends on the number of stacked cells and the power required (Brunetto; Moschetto; Tina, 2009).

Figure 1 – PEMFC Single Unit Cell Schematic

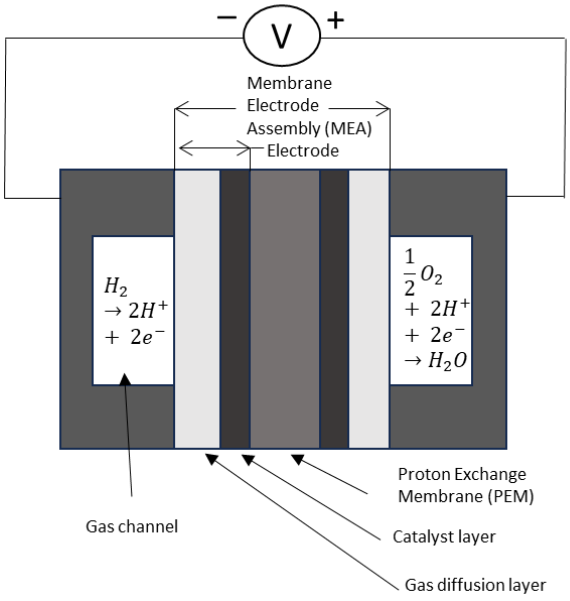

Source: (Litster; McLean, 2004)

The main advantages of PEMFCs are low or zero carbon emissions (depending on how the hydrogen is obtained), high energy efficiency, low temperature, and easy scalability of power and capacity (Kirubakaran; Jain; Nema, 2009; Taner, 2015) . As a result, they have been widely used in various application fields, such as portable devices, transportation, and cogeneration (Sharaf; Orhan, 2014). However, its low durability and high cost still hinder large-scale commercialization (Wang et al., 2021). According to the U.S. Department of Energy, the target cost for PEMFC is $30/kW and the durability target in an automotive cycle is 8000 hours. Current values are 76$/kW and durability of about 4000 to 5000 hours (Hua et al., 2022).

While there are many strategies to lower the cost of fuel cells (such as replacing or reducing the presence of noble metals in their components or through their high-volume manufacturing process (Bar-On; Kirchain; Roth, 2002)), their low durability and degradation process are not yet fully understood (Vichard et al., 2020). This is because there are many factors that can influence the degradation process of fuel cells, such as mechanical and thermal stresses, load demand variation profiles, humidity levels during operation and start/stop conditions (Jouin et al., 2013).

In this context, Prognostics and Health Management (PHM) represents a great opportunity to contribute to the extension of the lifetime of fuel cells (Kimotho; Meyer; Sextro, 2015). PHM is an engineering process that aims to improve the durability, reliability, safety, and cost-effectiveness of the system through a set of activities involving diagnostics and prognosis (Li; Verhagen; Curran, 2020; Sutharssan et al., 2015). This process makes it possible to assess the system’s current state in real operating conditions and improve its durability, predicting possible failures and carrying out the required maintenance procedures.

In the present work, we focus mainly on the prognostic part of PHM (Figure 2). According to the ISO 13381 Standard (Hitchcock, 2006), the prognosis "is an estimate of the time to failure and the probability of one or more existing and future failure modes". The prognosis aims to:

- Estimate degradation trends and determine factors influencing deterioration;
- Estimate the remaining useful life (RUL) of the system;

- Set an estimate confidence level.

Figure 2 – Prognostics methodology

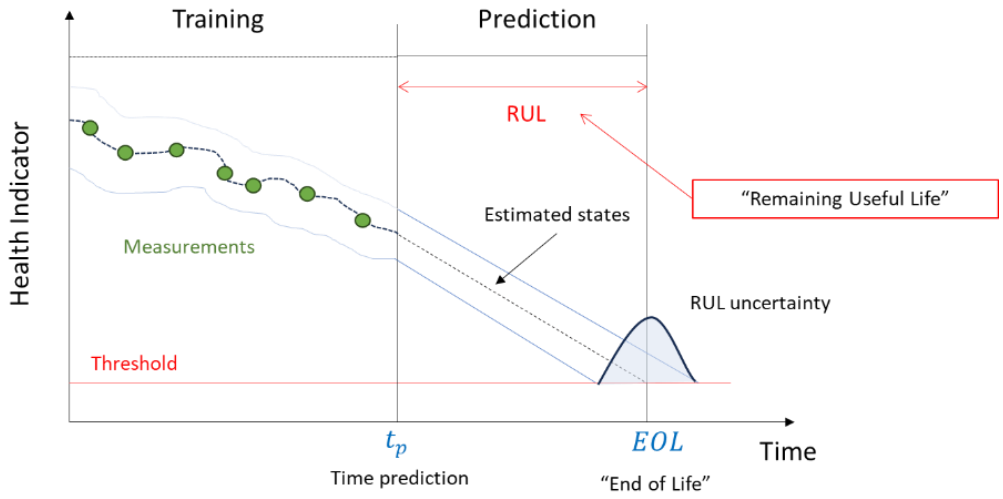

Source: (Yue et al., 2021)

The remaining useful life of the system Equation 1. is the time difference between when the prediction was made (t_p) and when the PEMFC cannot deliver the required power (t_f), i.e., the PEMFC reaches the end of life (EOL) (Jouin et al., 2014).

$$RUL = t_f - t_p \qquad (1)$$

Some authors (Jin et al., 2024; Peng et al., 2023; Yang et al., 2023) also propose a distinction between long-term prognosis and short-term prognosis based on how further away the future states of the system can be predicted. Since long-term prognostics often require several sequential estimates, giving room to prediction error accumulation, it is a more difficult task to be performed. Still, maintenance procedures require time to be scheduled and performed, being long-term prognosis more useful to the maintenance crew and therefore the focus of this project.

Therefore, the general objective of this work is to develop a hybrid thermodynamic model to predict long-term performance of the PEMFC and its tendency to degrade during its operation. The general objective is divided into the following specific objectives:

- Extend the Degradation Entropy Generation theorem (DEG theorem) to a prognostics approach using physics informed recurrent neural networks (PIRNN).
- Evaluate the energy conversion efficiency and fuel consumption of PEMFC over its lifetime;
- Predict the degradation trend and estimate the RUL based on the DEG theorem, which relates the degradation of PEMFC with the generation of entropy;

The literature presents the application of the DEG theorem in galvanic cells that are closed thermodynamic systems, such as batteries. We understand that the major contribution of the present proposal comes from the application of the DEG theorem to galvanic cells that are open thermodynamic systems, such as fuel cells and its extension to a prognostic model using physic informed recurrent neural networks.

The following sections are structured as follows: Section 2 presents the literature review of past prognostics methods and loads applied to them; Section 3 presents the methodology followed to apply the hybrid prognostic method; Section 4 presents the results obtained with it and Section 5 the final conclusions. For the interested reader the obtention of the entropy generation model for the PEMFC is also available at Appendix A.

2 LITERATURE REVIEW

Generally, there are three approaches to estimating the remaining lifespan of PEMFC: model-based methods, data-driven methods and hybrid methods (Hua et al., 2022). Data-driven methods use "black-box" models such as machine learning, deep learning, and statistical algorithms to learn system behavior directly from historical data, without the need to understand the complex physical interactions of fuel cells (Sutharssan et al., 2017). This approach is generally preferred over model-based methods because it provides accurate results when compared to test data and is easier to implement (Zhou et al., 2024).

Several researchers have used data-driven methods to estimate the remaining lifespan of PEMFC. Silva et al (2014) proposed the use of an adaptive neurofuzzy inference system (ANFIS) to predict the long-term degradation trend of two PEMFC stacks operating at constant load. The authors also proposed to separate the output voltage of the cells into normal operating voltage and external disturbance and using only the normal operating voltage to train the ANFIS. The validation results showed that the model was able to predict fuel cell degradation with a R^2 score above 0.95.

However, the ANFIS model uses an iterative structure that makes it accumulate errors and be computationally expensive. Therefore, Javed et al (2016) proposed the use of a set method to combine Summation Wavelet and Extreme Learning Machine (SW-ELM) models to obtain a more robust model to predict the long-term degradation of two different fuel cells operating at constant current. The authors also showed the importance of constraints in any connectionist method that deals with reduced measurements and the importance of the amount of training data for the accuracy of the models.

Morando et al (2017) introduced the use of the Echo State Network to predict fuel cell degradation from the IEEE PHM Data Challenge. The authors used a combination of wavelet transform and Hurst coefficient to filter out the output voltage of the stack and improve the model's prediction. Liu et al (2017) proposed a method that combines a group method of data handling (GHDM) network and Wavelet decomposition (W-GMDH) to predict short-term degradation in raw data. The method

was compared with a simple GMDH and showed that the use of Wavelet decomposition increased the accuracy of the model.

Ma et al (2018) introduced the use of Grid Long Short-Term Memory (G-LSTM) to predict the short- and long-term degradation of PEMFC. The G-LSTM model was compared with other methods based on literature data, the relevance vector machine (RVM) and the Elman Network, and the results demonstrated the superiority of G-LSTM.

The refs. (Javed et al., 2016; Liu et al., 2017; Ma et al., 2018; Morando et al., 2017; Silva et al., 2014) proposed an approach based on constant loads, which remains the same for the whole PEMFC lifetime. As observed in Figure 3, dynamic or semi-dynamic conditions represent better a real-world operation condition at which loads are typically varied.

Figure 3 – Types of load operation

Figure 3a – Constant load

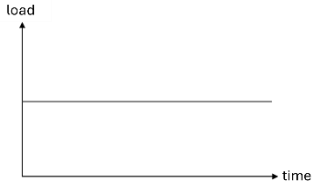

Source: author production

Figure 3b – Semi-dynamic load

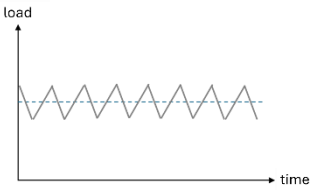

Source: author production

Figure 3c – Dynamic Load

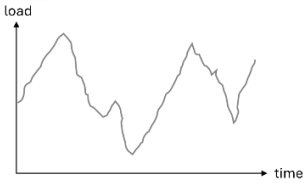

Source: author production

In this context, Wang et al (2023) proposed the use of a Hilbert-Huang transform (HHT) to extract health indicators from the dynamic output voltage, and then applied a Gated Recurrent Unit (GRU) neural network and an LSTM neural network to predict the RUL. The GRU method proved to be computationally cheaper than the LSTM and provided accurate results under different failure thresholds.

Even though references (Javed et al., 2016; Liu et al., 2017; Ma et al., 2018; Morando et al., 2017; Silva et al., 2014; Wang et al., 2023) got positive results, data-driven methods require large amounts of data to avoid overfitting problems and specialized knowledge to fit the hyperparameters of "state-of-the-art" models (Liu et

al., 2020). These factors make it very difficult to implement them in real-time operations, where working conditions can change from time to time. Also, because aging experiments are so expensive, there are not many datasets available for algorithms to train or validate. According to Yue et al (2021), by 2021, more than 60% of PEMFC prognostic methods used one data source, the IEEE PHM Data Challenge that took place in 2014.

On the other hand, model-based methods require less training data and better generalize the prognosis (Liu et al., 2020). In this type of method, physical, empirical or semi-empirical equations are used to predict the degradation of the system (Hua et al., 2022). In addition, because these methods are more based on the physics involved than data-driven methods, their results are often more informative to the user than "black-box" methods.

Several researchers have used model-based methods in the prognosis of PEMFC. Not just at the stack level, like most data-driven methods, but also at the cell and component level. Zhang and Pisu (2014) proposed a dissolution model of the catalyst particles to characterize the relationship between operating conditions and the electrochemical surface area degradation rate (ECSA), and then applied an unscented Kalman filter (UFK) for the prediction of the RUL. The results showed that the UFK algorithm can accurately predict the degradation of the ECSA and the PEMFC RUL.

Polverino and Pianese (2016) proposed a RUL estimation method based on an ECSA degradation model that considers the dissolution of the catalyst particles and the effect of Ostwald ripening. While the radius of the catalyst particles and ECSA can accurately reflect the degradation of PEMFC, these indicators can only be obtained in the laboratory.

In this context, Pan et al (2020) proposed an equivalent circuit model (ECM) to estimate the electrochemical impedance spectroscopy (EIS) of the fuel cell. The method demonstrated that EIS indicator can be used to reflect degradation not only on a macro scale but also help acquire information at the component level. The model was able to estimate voltage drop and recovery accurately, but the ECM parameters need to be initialized after cell operation, which makes this method unfeasible for real-time applications.

Bressel et al (2016) proposed degradation models for internal resistance and limit current combined with an Extended Kalman Filter (EFK). Chen et al (2022)

proposed models of ECSA degradation mechanisms, leakage current, internal resistance, and limit current with a particulate filter method to predict the RUL of PEMFC operating at constant load. The results showed that ECSA thinning was the main cause of the decay of performance over the life of the cell, but the leakage current increased near the EOL.

The accuracy of model-based methods, however, depends heavily on the limitations of the model to capture the physical interactions of the fuel cell (Yue et al., 2021), which are not yet fully understood and need to be further developed.

Considering the advantages and limitations of data-driven and model-based methods, some authors created hybrid models that combine both approaches. Tian et al (2023) proposed an empirical voltage recovery model and bayesian optimization of a multi kernel relevance vector machine (VR-BO-MK-RVM) method to predict both the cell's voltage degradation and its recovery after the characterizations. The method presented an RMSE of 6.9 mV.

Since the method was developed to predict only short-term degradation, it was not suitable to estimate the RUL. Therefore, Wang et al (2022) proposed a LSTM-gaussian process regression (LSTM-GPR) for short term prediction and a combination of an Extended Kalman Filter (EKF) with a Gaussian Process Regression (GPR) for long term prediction.

Ma et al (2021) developed a physical model of aging to capture the degradation of the internal components of PEMFC: an EFK, to handle the nonlinear characteristics of the fuel cell with a fast computational speed; and an LSTM, to capture the trend of the output voltage and obtain more accurate prediction results.

Outside the area of prognosis, some researchers have proposed thermodynamic models to analyze the degradation and economic impacts of PEMFC operating conditions. Chen et al (2021) presented a PEMFC degradation model to compare four different constant currents of operation. The results showed that the model adjusted well to the polarization curves and that at a higher current the degradation rate, power capacity, fuel consumption and overall cost increase. However, the authors did not consider the effects of cell stacking in the model and validated it at constant currents that do not reflect the actual dynamic functioning of the fuel cells.

Xu et al (2023) proposed a similar degradation model and then applied an optimization algorithm to find the best operating conditions of PEMFC. The authors were able to minimize the degradation rate by nearly 42 percent and the cost by 31 percent through a combination of low current, low electrical power, high hydrogen gas pressure, and low temperature.

Qureshy et al (2022) analyzed the impact of different environmental conditions on the degradation of PEMFC and stated that, although different environmental temperatures did not directly affect the temperature of the fuel cell (due to the presence of coolers), their effects on the relative humidity of the air cause a decay of the charge transfer of the fuel cell.

These results are useful to understand how operating conditions impact the degradation and, consequently, the cost of the fuel cell. However, the results were obtained under specific laboratory conditions and can hardly help the decision-making process under different operating conditions, requiring prognostic approaches.

A concept widely used within the field of thermodynamics to model energy losses in real systems is the concept of irreversible entropy generation $\delta S'$. Through the Gouy-Stodola theorem (Equation 2), the rate of entropy generation is used to model the energy losses that an irreversible (real) operating system has in relation to a system operating in a reversible (ideal) way. In Equation (2), T is the temperature, δW_{rev} is the reversible work, which can be understood as the maximum theoretical work possible to be done, and δW is the actual work.

$$T\delta S' = \delta W_{rev} - \delta W \geq 0 \tag{2}$$

Bryant et al (2008) proposed that this concept should also be used to model the degradation of systems, through the Degradation-Entropy Generation Theorem (DEG). This theorem establishes a direct relationship between a measure of degradation w and rates of irreversible entropy generation dS_i'/dt for each irreversible transformation i (Equation 3). According to Osara and Bryant (2019a), "entropy measures the disorganization of a system. Since degradation is advanced and permanent disorganization, the generation of entropy is fundamental for the evaluation of the degraded system."

$$\frac{dw}{dt} = \sum_i B_i \ \frac{dS_i{}'}{dt} \tag{3}$$

In Equation 3, the parameter B_i represents a property of the systems defined by the gradients of w in relation to the generation of irreversible entropy $S_i{}'$ for each active dissipative process p_i (Equation 4). A dissipative process p_i refers to a form of energy dissipated by internal processes, such as loss of work, heat transfer, or a change in thermodynamic potentials (internal energy, enthalpy, Gibbs' or Helmholtz's free energy).

$$B_i = \left.\frac{\partial w}{\partial S_i{}'}\right|_{p_i} \tag{4}$$

The steps of applying the DEG theorem are described below:

1. Identify a measure w that reflects degradation over time. This measure should be positive and grow over time.
2. Through the knowledge of degradation mechanisms, identify dissipative processes $p_i = p_i(\zeta_{ij})$ that represent energy losses and the phenomenological variables ζ_{ij} that characterize these losses.
3. Obtain the entropy generation rate dS_i'/dt through the application of thermodynamic modeling of $p_i(\zeta_{ij})$.
4. Determine B_i and use Equation 2 to get an expression for the degradation rate dw/dt.

The application of the DEG theorem is in accordance with other approaches in literature(Bryant; Khonsari; Ling, 2008). Considering the example of the interfacial wear between solids due to sliding friction (Bryant; Khonsari; Ling, 2008), the rate of wear obtained through the DEG theorem is $\dot{w} = B\eta\dot{x}N/T$, where η is the coefficient of friction, $\dot{x}$ is the sliding velocity, N is the normal force and T is the temperature. The phenomenon is governed by Coulomb's law of friction ($F = \eta N$) and Archad's law of wear ($\dot{w} = k\dot{x}N/H$), in which H is the hardness of the most brittle material. Comparing the rate of wear obtained by the DEG theorem with Archad's law of wear, we have that $B = kT/\eta H$. Doelling et al (2000), through an experimental B, obtained a value of k similar to that obtained by the Rabinowicz method.

The DEG theorem has been applied in several domains, with promising results in degradation state evaluation, such as friction wear modeling (Bryant; Khonsari; Ling, 2008), lubricant degradation (Osara; Bryant, 2019c), fatigue failure (Osara; Bryant, 2019b), abrasive wear and combined adhesives (Lijesh; Khonsari, 2020), and voltage drop of lead acid (Osara; Bryant, 2019d) and lithium-ion batteries (Osara; Bryant, 2019a). Nevertheless, it has not been applied yet to PEMFC prognostics or combined with physics informed neural networks recently proposed by Raissi et al(2019).

3 MATERIALS AND METHODS

The prognostic methodology used in this work is broken down into the following methodological steps: aging experiment, health indicator definition, data preprocessing, degradation model development, model training and validation, EOL definition and RUL prediction and evaluation.

3.1 AGING EXPERIMENT

Aging experiments provide data for the model to be trained and validated. The experiment aims to replicate a real fuel cell operation as closely as possible, without losing any data to be collected. As stated in section 3, the aging experiment that is most utilized in the literature is the IEEE PHM 2014 Data Challenge ("dat@UBFC : IEEE PHM Data Challenge 2014", 2014). This is an open-source dataset provided by FCLAB, in which two PEMFC stacks were selected for degradation tests: FC1 and FC2, operating under constant load of 0.7 A/cm^2 and semi-dynamic load of 0.7 A/cm2 with triangular ripples of 0.14 A/cm^2, respectively, for 1000 hours. Both stacks consisted of five cells, each with a uniform active cross-sectional area of 100 cm2, with nominal and maximal current densities of 0.7 A/cm2 and 1 A/cm2, respectively, resulting in a maximum total power of 1 kW.

Figure 4 – IEEE 2014 PHM Data Challenge cells operation

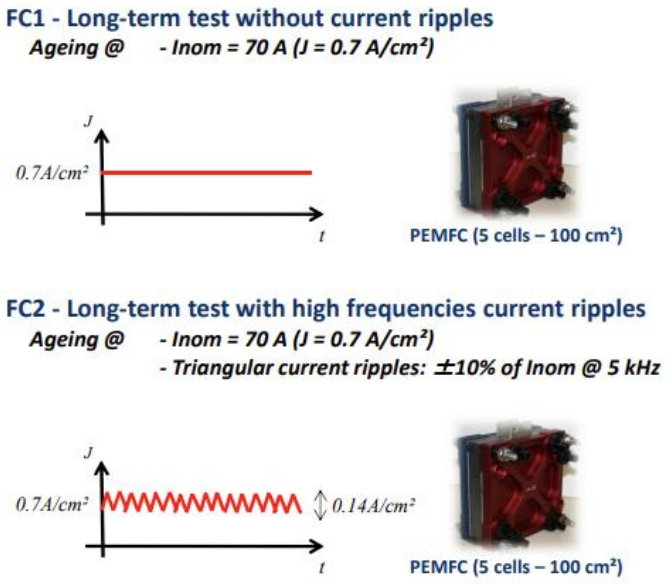

Source: (“dat@UBFC : IEEE PHM Data Challenge 2014”, 2014)

The operating information available in the dataset are current, individual cell voltage, cooling water flow rate and inlet and outlet temperature, gases (air and hydrogen) inlet and outlet temperatures, pressures, volumetric flows and the estimated inlet hygrometry of the air. In addition, polarization and impedance data were also measured weekly through characterizations tests such as the polarization test and the electrochemical impedance spectroscopy. The polarization curves and the Nyquist plot for FC1 are shown in Figures 4 and 5.

Due to the challenge characteristics of the dataset, at which FC1 data was intended to be used as training data, half of FC2 data to be used as test data and the other half to evaluate the candidates. Only part of the characterization data from FC2 was made public available (until 515h).

Figure 5 – Polarization curves of FC1 from IEEE PHM 2014 Dataset

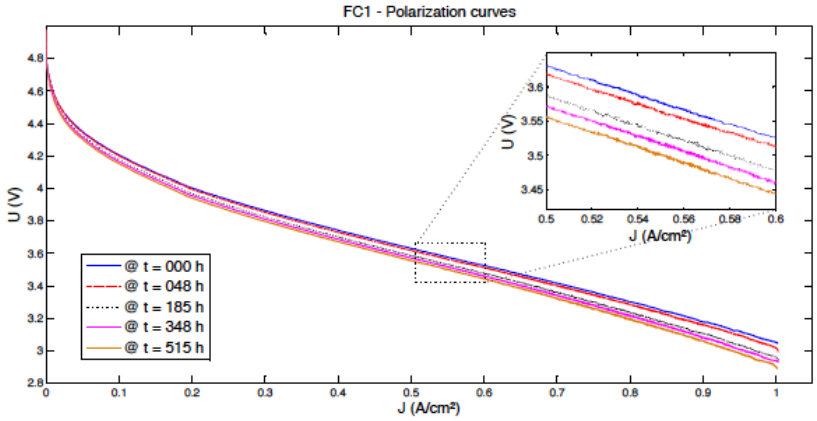

Source: (“dat@UBFC : IEEE PHM Data Challenge 2014”, 2014)

Figure 6 – Nyquist plots of FC1 from IEEE PHM 2014 Dataset

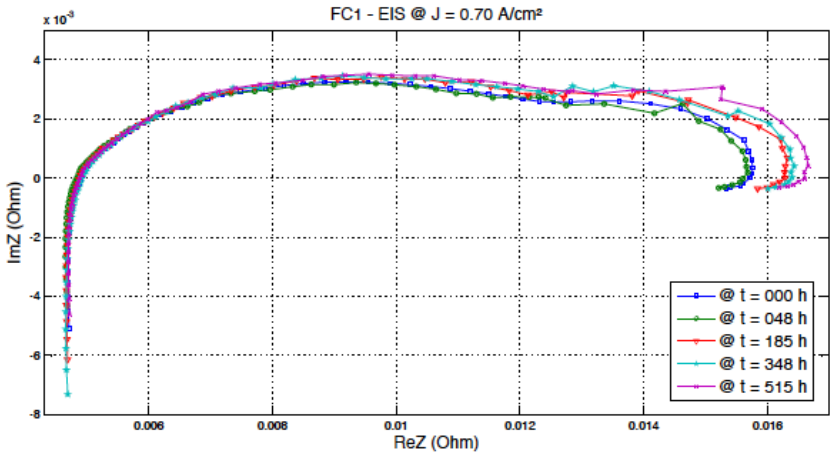

Source: (“dat@UBFC : IEEE PHM Data Challenge 2014”, 2014)

3.2 HEALTH INDICATOR

There is a variety of health indicators (HIs) available to be used in PEMFC prognostics context (Ao et al., 2021; Chen et al., 2022; Hua et al., 2020; Yu et al., 2024a), but since the DEG theorem treats degradation as an irreversible accumulative disorganization process, it expects an always increasing (or decreasing) HI. As observed in Figure 7, the stack operating voltage shows clear signs of recovery during the cell lifetime, especially during the characterization process, when the fuel cell usually rests before the characterization is performed. This recovery process when the cell is not being operated can be explained by several reasons such as the rearrangement of the ions in the membrane electrode assembly (MEA) and the humidity conditions in the electrolyte, still it is not fully understood and represents a challenge in modelling approaches.

Figure 7 – IEEE PHM 2014 voltage decay

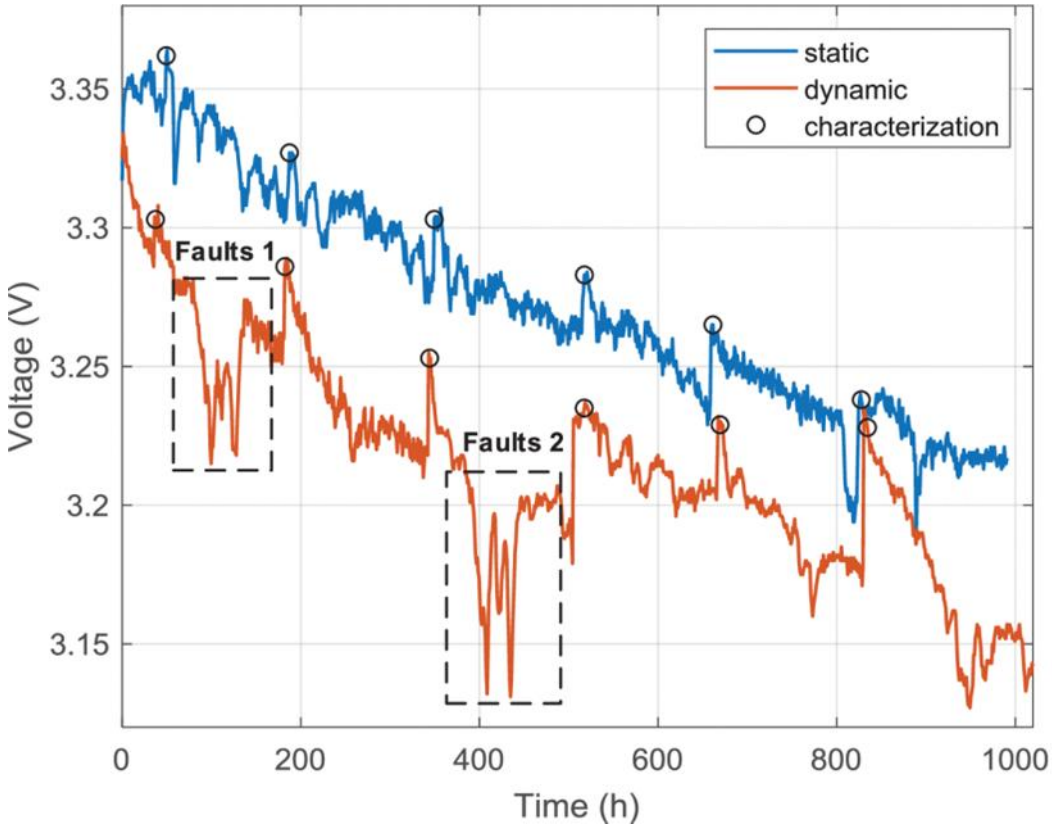

Source: (Li et al., 2024).

The polarization curves, on the other hand, follow the irreversible decay phenomenon and therefore were chosen as the HI for the prognostic. In order to reduce the computational burden in the model but still represent the overall polarization decay of cell, 4 polarization points were chosen (1A, 3A, 50A and 70A). As shown in Figure 8, these points will represent the overvoltage predominant in each load condition of the cell:

- Activation Overvoltage η_{act} , which accounts for reaction kinetics losses at electrode/electrolyte interfaces, are the predominant voltage losses for low current values.
- Ohmic Overvoltage η_{ohm}, which accounts for the transport of H^+ losses at the electrolyte, are the predominant voltage losses for medium load conditions.
- Concentration Overvoltage η_{conc} , which accounts for reactants concentration losses at electrodes, are the predominant voltage loss for higher load conditions. At this operation mode, the gas pressure at the

electrodes, especially at the cathode, limit the concentration of the reactants that reach the MEA of the cell.

Figure 8 – Points 1A, 3A, 50A and 70A chosen as health indicators

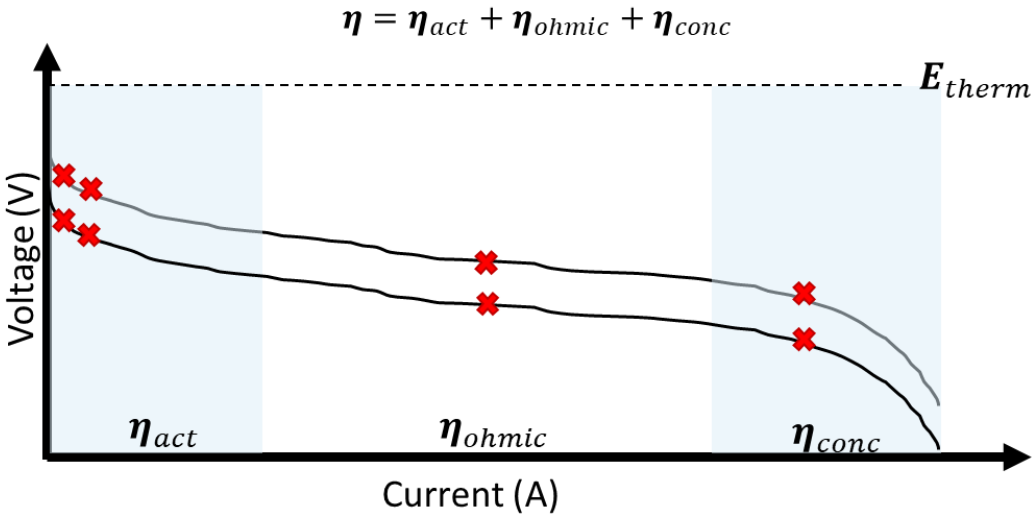

Source: (author production).

In addition, since the entropy generation of gases is not a function of the current load condition i, another degradation indicator can be defined: the gas e consumption efficiency ε_e (Equation 5), where dq is the change in charge, n the stoichiometry factor, F the Faraday constant and dN_e the change in mols of gas e.

$$\varepsilon_e = \frac{dq}{nF dN_e} \tag{5}$$

This indicator relates to the number of electrons generated per amount of gas consumed. In an ideal condition, where side reactions are not present, 1 mol of hydrogen and half mol of oxygen gas would generate 2 mols of electrons following oxidation and reduction reactions on the electrodes (Equation 6 and 7).

$$H_2 \rightarrow 2H^+ + 2e^- \tag{6}$$

$$2H^+ + 2e^- + \frac{1}{2}O_2 \rightarrow H_2O \tag{7}$$

3.3 DATA PREPROCESSING

In order to prepare the data to train the DEG-PIRNN model, the moving average filter was applied to remove the noise and the outliers present in the dataset. In addition, the Pyromat library (Ranalli et al., 2022) was used to obtain the thermodynamic properties of the gases as functions of their pressure and temperature. From the gases properties and the overvoltages, the entropy generation rate is calculated through Equation 8.

$$\frac{\delta S'}{dt} = \frac{h_{reac} dq}{2TF} + \sum \frac{h_{e,exit} dm_e}{TMM_e dt} + \frac{(\eta_{act} + \eta_{ohmic} + \eta_{conc}) dq}{Tdt} - \frac{LHV_{H2} dm_{H2}}{Tdt} \quad (8)$$

In Eq 8, $\delta S'$ is the entropy generation, dt is the time change, h_{reac} the enthalpy of the full reaction, T is the temperature, $h_{e,exit}$, dm_e and MM_e are, respectively, the gases e enthalpy, change in mass and molar mass; and LHV_{H2} are the lower heating value of the hydrogen. The thorough derivation of Equation 8 is available in Appendix A.

The main assumptions used to obtain Equation (10) are listed below:

- Local equilibrium: even though the PEMFC is not at equilibrium at the macro scale, each infinitesimal control volume inside the cell is at equilibrium;
- Heat is generated/absorbed through the following mechanisms: ionic resistivity at the membrane, electrochemical reactions at catalysts, absorption/desorption of water at the membrane, overvoltages at the electrodes;
- Electrode reactions are perfectly coupled;
- All the water produced by the cell is expelled;
- The overvoltage of the cell η is only due to activation η_{act}, ohmic η_{ohmic} and concentration η_{conc} losses.

The entropy generation rate is integrated using Scipy integration function (Virtanen et al., *[S.d.]*). The data is then resampled to an hour interval and shifted using

a rolling window method with a 150 h shift between its inputs and target data before it is fed to the model.

3.4 DEGRADATION MODEL

The physics informed recurrent neural network (PIRNN) model developed is exhibited in Figure 9.

Figure 9 – Degradation Entropy Generation Physics Informed Recurrent Neural Network (DEG-PIRNN) schematic

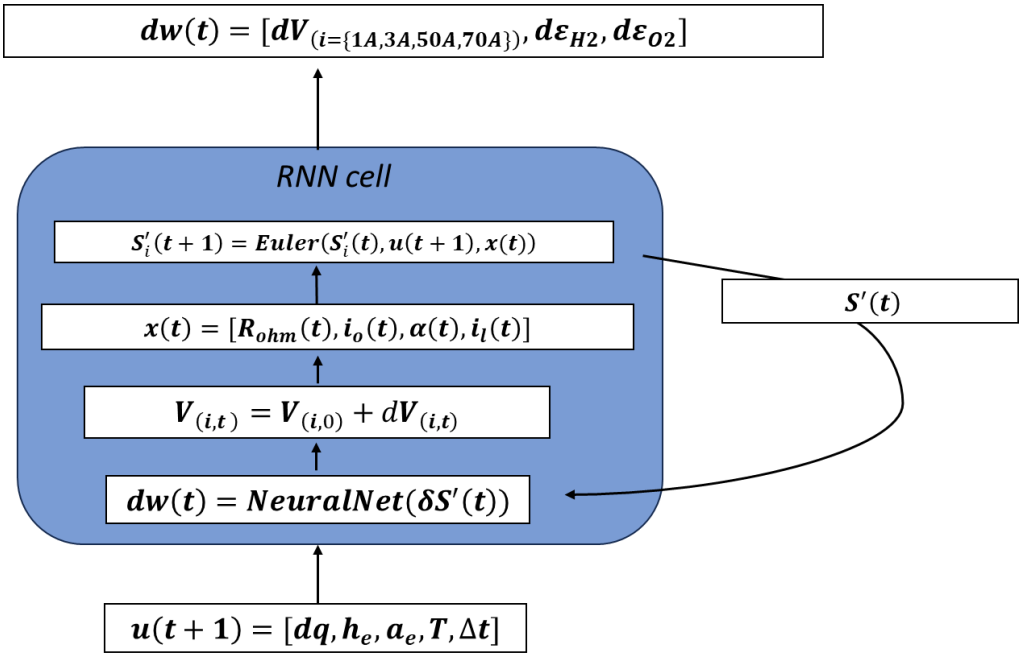

Source: (author production).

The RNN cell receives as inputs the entropy generated until time t and the controlled variables at time step $t+1$. It predicts the degradation indicators $dw(t)$, which consists of the decay of the four polarization points mentioned in Section 4.2 and the gases efficiency $\varepsilon(t)$. From the polarization decay $dV(i,t)$, it obtains the current polarization values $V(i,t)$ which is then used to obtain the internal state variables $x(t) = [R_{ohm}(t), i_o(t), \alpha(t), i_l(t)]$ through Equation. 9-11.

$$\eta_{act} = \frac{RT}{\alpha nF} ln(i) - \frac{RT}{\alpha nF} ln(i_o) \quad (9)$$

$$\eta_{ohm} = R_{ohm} i \quad (10)$$

$$\eta_{conc} = \frac{RT}{nF}\left(1 + \frac{1}{\alpha}\right) ln\left(\frac{i_l}{i_l - i}\right) \quad (11)$$

At which R is the ideal gas constant, α is the reaction symmetry coefficient, i_o is the exchange equilibrium current, R_{ohm} is the fuel cell electrolyte resistance and i_l the limiting current. Equations 9-11 are applied using the following procedure:

1. Using the assumption that only η_{act} is present at small loads, $i_o(t)$ and $\alpha(t)$ are obtained using Equation 9 and the first two polarization points chosen.
2. Using the assumption that only η_{act} and η_{ohm} are present at medium loads, R_{ohm} is obtained using the previously obtained values of $i_o(t)$ and $\alpha(t)$, Equations 9 and 10 and the third polarization point chosen.
3. At high load conditions, all overvoltages affect the PEMFC potential and i_l is obtained using Equations 9-11 alongside the previous parameters and the fourth characterization point.

Equation 8 is then applied to obtain the entropy generation during the interval Δt, which is then summed with $S'(t)$ to obtain $S'(t+1)$.

3.5 MODEL TRAINING

In order to train the model, the data from the IEEE 2014 PHM dataset was split into two: the data from FC1 was used to train and validate the model hyperparameters and data from FC2 was used to evaluate the prediction results. The model weights were initialized with zeros and were trained (optimized) for 10.000 epochs (training iterations) using the loss function exhibited in Equations 12-15 and the hyperparameters from Table 1 – Hyperparameters of the model

.

$$L_{DEG} = w(t) - \sum \frac{\partial w}{\partial S} S'(t) \quad (12)$$

$$L_{elech} = Relu(\alpha - 0.999) + Relu(0.0001 - \alpha) \quad (13)$$

$$L_{char} = w(t) - w_{pred}(t)) \quad (14)$$

$$L_{data} = S'(t) - S'_{pred}(t)) \quad (15)$$

$$L_{model} = RMSE(w_{deg}L_{DEG} + w_{elec}L_{elech} + w_{char}L_{char} + w_{data}L_{data}) \quad (16)$$

The loss function combines the data losses due to the entropy generation that are always available, the boundary losses that are available occasionally, when characterization tests are performed, and a physics loss composed by the DEG theorem and arbitrarily chosen electrochemical loss that enforces the symmetry coefficient to stay within real values. Since the DEG theorem is a partial differential equation, the auto differentiation property of neural networks was used here to enforce Equation 3, similarly to what was done by Raissi et al (2019).

Table 1 – Hyperparameters of the model

hyperparameter	$\boldsymbol{value}$
$learning\ rate$	$1e^{-4}$
$epochs$	10.000
$patience$	500
w_{deg}	0.5
w_{elec}	1
w_{char}	1000
w_{data}	1

To prevent the characterization loss from being neglected during training due to limited data, a higher weight was arbitrarily assigned to it.

3.6 MODEL EVALUATION

In order to evaluate and compare the model predictions with the data two metrics are used: the R squared (Equation 17)) and the root mean squared error (Equation 18).

$$R^2 = 1 - \frac{SS_{res}}{SS_{tot}} \tag{17}$$

$$RMSE = \sqrt[2]{\frac{1}{n}\sum (y_i - \hat{y}_i)^2} \tag{18}$$

A benchmark model is considered to compare the accuracy of the new method to the ones usually found in literature. The benchmark model was developed by Bressel et al (2016), who proposed a model-based degradation method based on a polarization model combined with an Extended Kalman Filter (EKF). The model predicted the PEMFC degradation based on the increase of the ohmic resistance R_{ohm} (Equation 19) and decrease of current i_l (Equation 20), who were obtained by fitting the model to experimental data. Both parameters were later related to a degradation parameter α_{degr}, which was advanced through time to predict the RUL.

$$R_{ohm}\,(t) = R_{ohm}\,(1 + \alpha_{degr}(t)) \tag{19}$$

$$i_l\,(t) = i_l\,(1 - \alpha_{degr}(t)) \tag{20}$$

3.7 END OF LIFE DEFINITION

As observed in Equation 1, the EOL is the threshold time at which the cell is considered failed. Even though the US Department of Energy has defined a 10% power decay for PEMFC, different authors considered different thresholds depending

mostly on the HI utilized and the load conditions (Liu et al., 2024; Wu et al., 2024; Yu et al., 2024b).

Since there are not many characterization points available from the test set to define an end of life, we used here two different indicators to predict the remaining useful life of the PEMFC and evaluate the model prediction capabilities:

- A 3% decay of the 70A polarization point (the same current that the cell is being operated).
- Maximum entropy generation due to the PEMFC overvoltages.

3.8 REMAINING USEFUL LIFE PREDICTION AND EVALUATION

In this step, the model iterates through the data to predict the remaining useful life of the fuel cell, i.e., how much time the fuel cell would take until reaches its end of life EOL.

The Prognostic Horizon (PH) metric is used to obtain how far away the model can predict within a precision accuracy threshold. As illustrated in Figure 10, the PH is obtained by (i) comparing the real RUL and the predicted RUL at different prediction times and (ii) defining a Trust Area (TA), which is the area between the upper/lower acceptable error boundaries parallel to the actual RUL. After a certain prediction time, the predicted RUL will all be located within the TA, and thus, it is possible to indicate how long ago the acceptable prediction could be obtained and ensured. The PH is calculated using Equations 15 and 16.

Figure 10 – Prognostic Horizon illustration

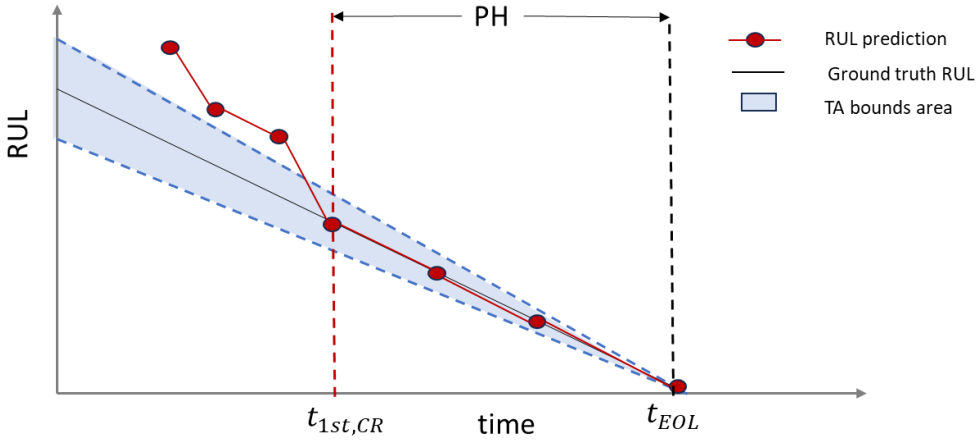

Source: (author production).

$$t_{1st,CR} = \min\{t\ e\ T \mid RUL - TA_l EOL \leq RUL_{pred}(t) \leq RUL + TA_u EOL\} \quad (21)$$

$$PH = EOL_{real} - t_{1st,CR} \quad (22)$$

In Eqs 15-16, $t_{1st,CR}$ is the first time at which the systems reach the EOL criteria defined in section 4.7, TA_{lower} and TA_{upper} are the trusting area bellow and above the real RUL (RUL_{real}) and RUL_{pred} the RUL predicted by multiple iterations through the model.

In order to showcase the usefulness of the entropy generation due to PEMFC overvoltage in prognostic horizon evaluation, a stricter margin than the polarization point decay is imposed. Thus, it is considered a 10% margin for the lower and upper bound of the first EOL criteria and 20% margin for the second one.

4 RESULTS

The results for the optimization of the neural network weights during the training are exhibited in Figure 11. As observed in the figure, even though the model was able to converge to a local minimum, occasional spikes occurred at early training epochs. A possible explanation could be the addition of the physics loss function used to enforce the symmetry coefficient to be within real physical bounds. When the model predicts an alpha smaller than zero or greater than one, the loss function will suddenly increase.

Figure 11 – Model training

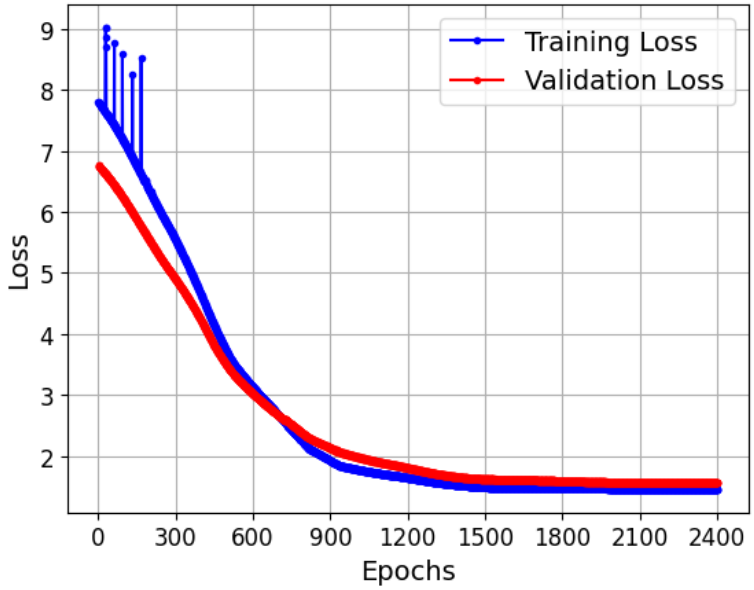

Source: (author production).

The results for the entropy generation prediction are exhibited in Figure 12. The entropy generation exhibits a linear trend, and therefore, is easily predicted by the model with all predictions reaching $R^2 = 1$. It can also be observed that FC2 has a higher entropy generation rate then FC1, which indicates that dynamic loads degrade the fuel cell capacity to convert energy faster than constant load conditions, making FC2 reach the EOL earlier than FC1.As observed in Osara and Bryant (2019a), the hyperplane formed by the entropy generation lines and the health indicator describe the possible paths that a system can take towards degradation. The higher the inclination of the planes, the faster the degradation is.

Figure 12 – Entropy generation prediction versus calculated

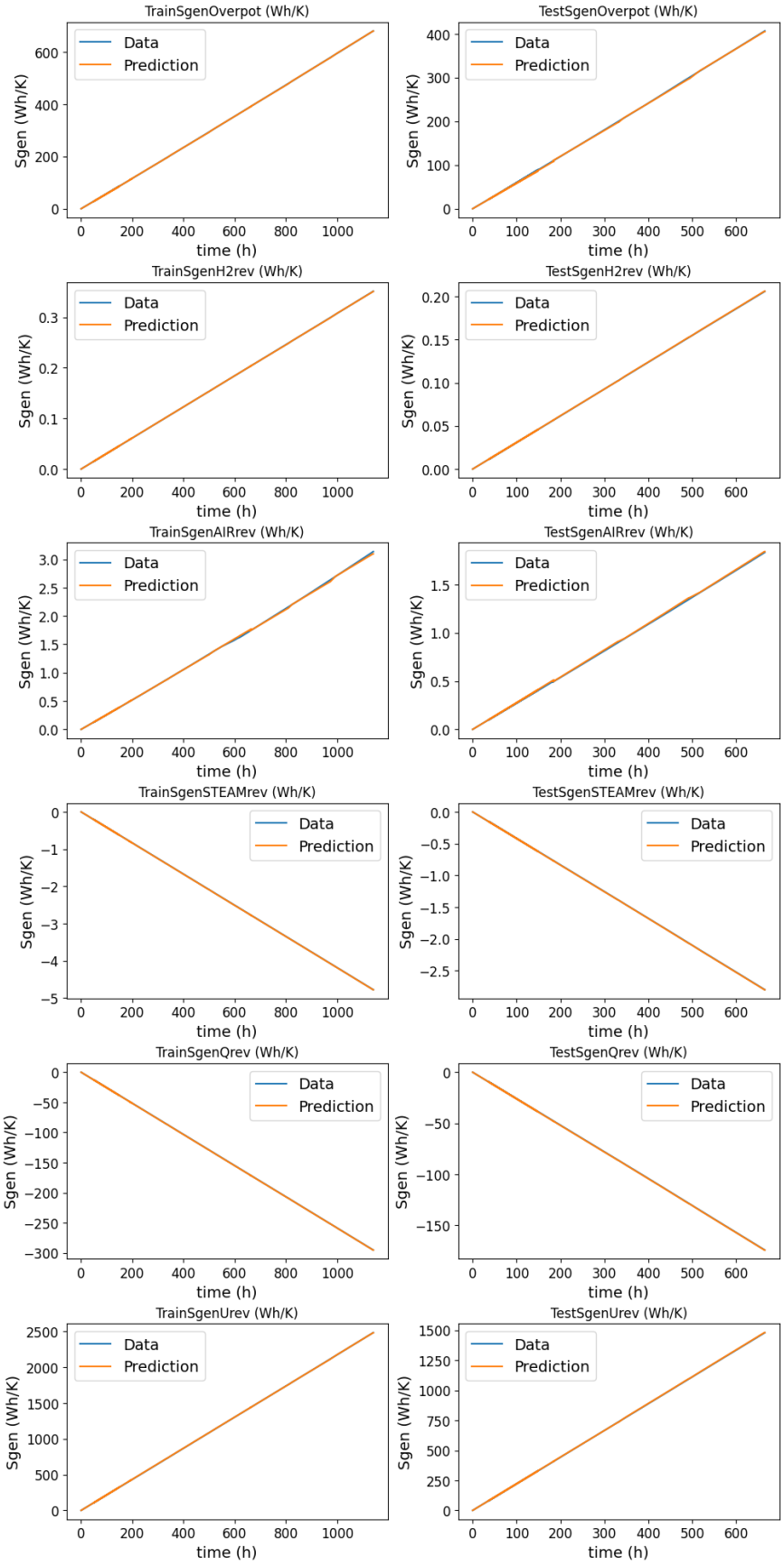

Source: (author production).

Legend: Entropy generation prediction versus calculated for train (left) and test (right) sets for each process happening inside the PEMFC. In order: SgenOverpot is the entropy generation due to PEMFC overpotentials, SgenH2rev is the entropy generation due to hydrogen consumption, SgenAIRrev is the entropy generation due to air consumption, SgenSTEAMrev is the entropy generation due to water consumption, SgenQrev is the entropy generation due to heat exchange and SgenUrev is the entropy change associated with internal energy change (author production).

The polarization points (1A,3A, 50A and 70A) predictions are shown in Figure 13. The model obtained a test root mean squared error (RMSE) of 16mV, 5mV, 15mV and 12mV, respectively. As observed, the model is capable to predict the degradation trend to all the points for both datasets. Similarly to what was observed in (Zhang et al., 2020), the model predicts a linear-exponential decay which indicates that, eventually, the cell will reach a maximum degradation and then stop degrading. It can also be noticed that the model is more precise for medium to higher loads, probably due to the operation load in the aging experiment being 70A.

Figure 13 – Polarization points (1A, 3A, 50A, 70A) decay prediction versus measurement for 150h ahead

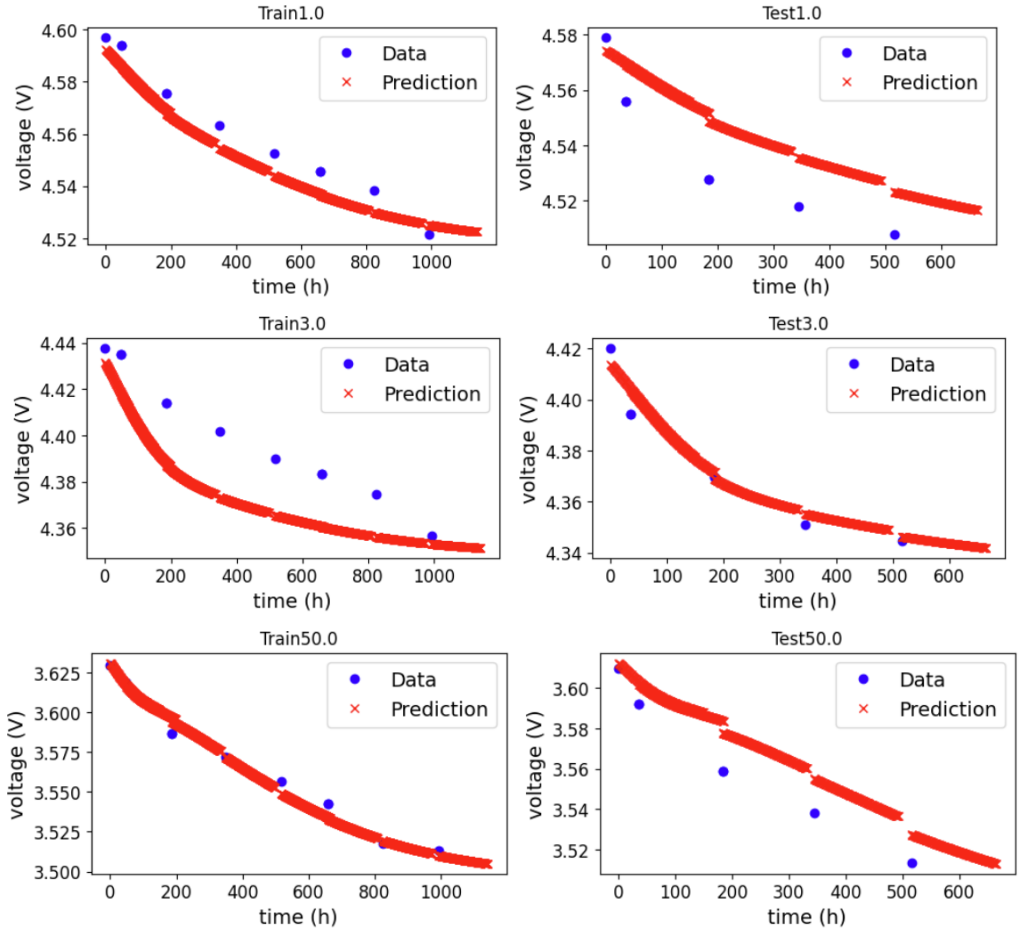

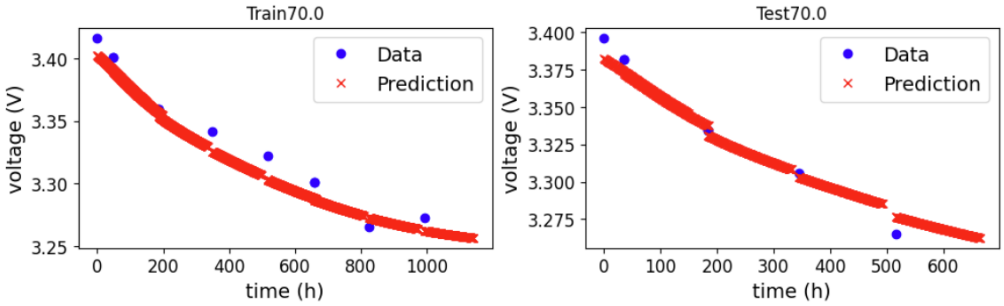

Source:(author production).

Table 2 – Polarization points train and test error

	TRAIN		TEST	
current (A)	RMSE (mV)	R^2 (%)	RMSE (mV)	R^2 (%)
1	7.6	89.9	16.7	49.3
3	20.8	35.1	5.9	94.1
50	6	97.5	15.6	75.4
70	12.1	94	8.6	96.1

Source:(author production).

The comparison of the DEG-PIRNN model (red) to the EKF model proposed by Bressel et al (2016) (green) for the polarization point 70A is shown in Figure 14. As observed, the hybrid approach proposed here outperforms the generalization and long-term prediction of the model-based one, especially for the test set where it got a prediction 86% more accurate (RMSE of 8.6mV versus 58.6mV). This result showcases the advantages of the hybrid method, which is not only easier to be trained for different conditions but also more accurate.

Figure 14 – Comparison with benchmark model for 70A polarization data

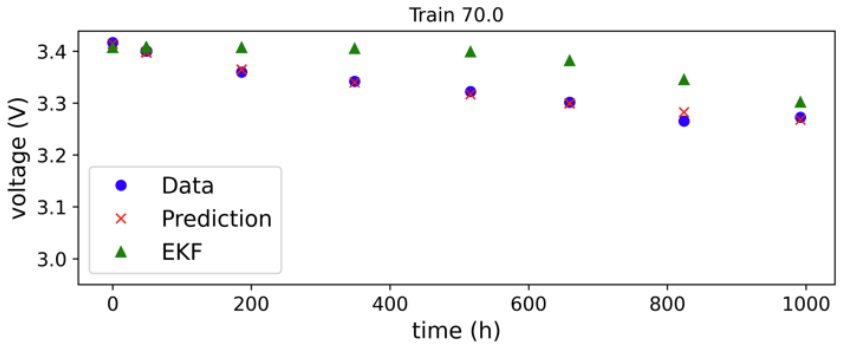

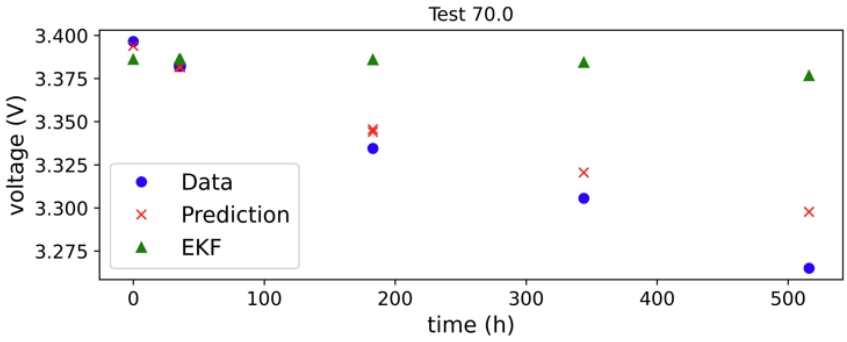

Source:(author production).

By using the PEMFC electrochemical parameters, the model was also able to predict different polarization points that have not been fed to it during the training such as (2A, 4A, 20A and 40A.) The polarization curves prediction is shown in Figure 15. As observed, the 150h ahead prediction can be performed with high accuracy, even for unseen data points with an RMSE of approximately 27mV. These results showcase the advantage of the hybrid approach when compared to a purely data-driven one, where unseen data points are not able to be predicted with high accuracy due to overfitting problems.

Figure 15 – Polarization curve prediction versus data for train and test set

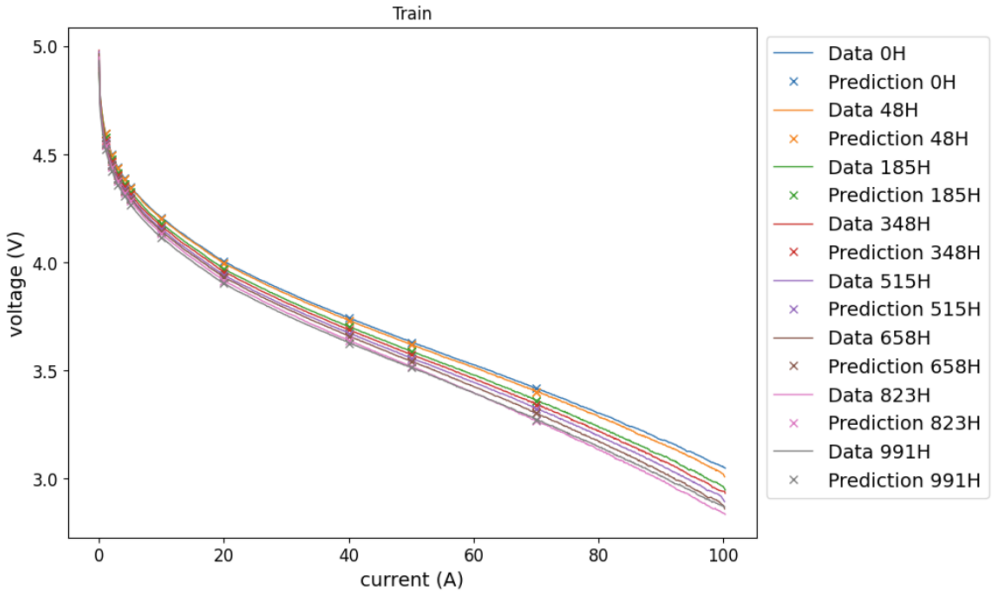

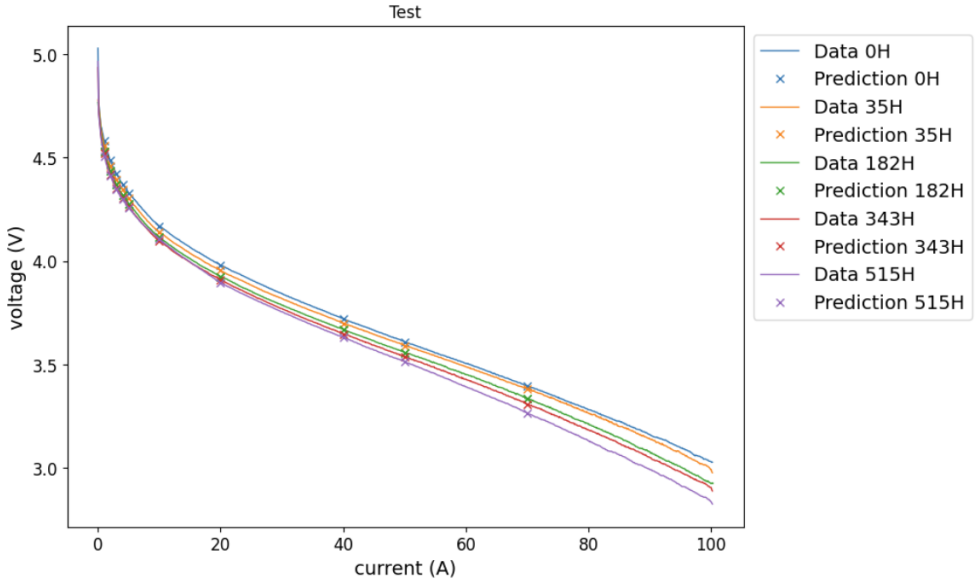

Source: (author production).

The hydrogen consumption (Figure 16) efficiency was successfully predicted for both the training and test datasets with an RMSE of 0.11 and 0.12 respectively; however, this was not the case for the oxygen. As shown in Figure 17, the decay in oxygen efficiency exhibits a different trend in the test dataset than what is observed on the training set, making it difficult for the model to predict it accurately. A possible explanation for that could be the occurrence of side reactions on the semi-dynamic dataset. Those side reactions would increase the consumption of oxygen without any current generation. Even more, it was stated in (Li et al., 2024) that the occurrence of faults in water management for FC2 could lead to inaccuracies in predicting its behavior. Therefore, it is suggested that a new model-based method relating water management with oxygen consumption should be incorporated in the hybrid-method proposed here to increase its generalization capabilities regarding this metric.

Even more, it can also be noticed that the efficiency of hydrogen consumption increases while oxygen decreases. This result is in accordance with the literature. As the cell ages, oxygen consumption increases due to a decrease in the diffusion process in the cathode and the presence of side reactions. Hydrogen, on the other hand, is not removed, increasing the concentration gradients opposed to the movement of hydronium ions within the cell, thus decreasing their consumption.

Figure 16 – Hydrogen consumption efficiency predictions

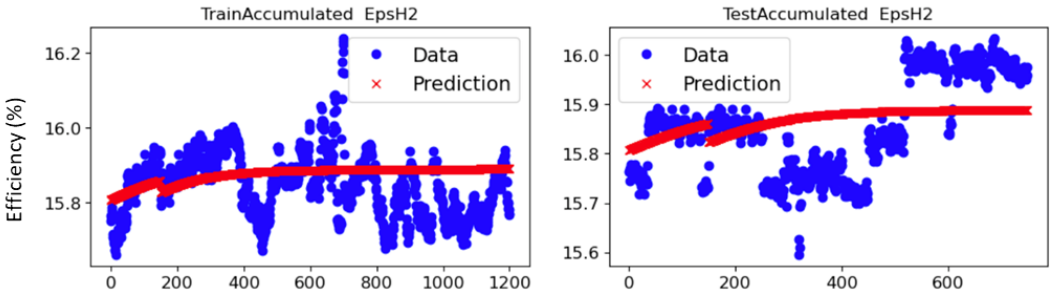

Source: (author production).

Figure 17 – Air consumption efficiency predictions

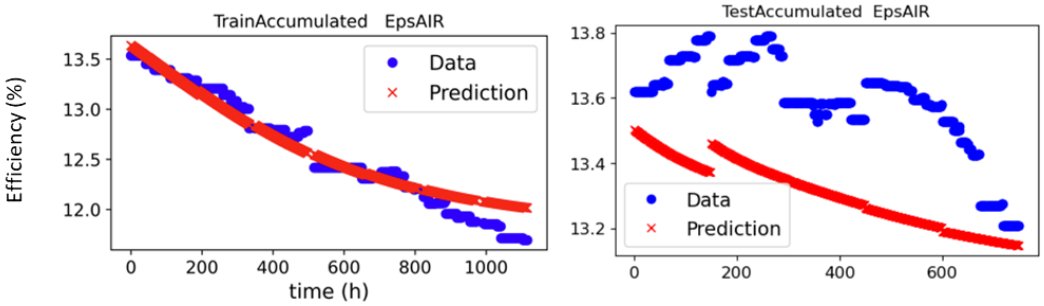

Source: (author production).

Using the auto differentiation process available in Tensorflow the gradients relating the decay of polarization points 3A and 70A to each entropy generation were also obtained (Figure 18). As expected, it can be noticed that the entropy generation due to the overvoltage $S'_{overpot}$ (blue) has a large negative relation with the health indicator. The higher the overvoltages, the lower the polarization curves.

It can also be noticed that the gradients of the entropy generation of the air $\delta S'_{air}$ (green) and hydrogen $\delta S'_{H2}$ (yellow) consumption have opposite signs. As previously discussed, higher hydrogen consumption is a good indicator of a healthy PEMFC, meaning that the oxidation-reduction reaction is performing as expected while a higher oxygen consumption can be either an indication of problems in diffusion processes in the cathode or the presence of side reactions, such as hydrogen peroxide formation.

The entropy generation term related to the maximum energy change in the cell $\delta S'_{Urev}$ showed a positive relationship with the polarization points. As observed in

(Castelino et al., 2023), a higher fuel pressure to the cell extends its lifetime by preventing fuel starvation.

The last two entropy generation indicators, related to the heat generated by the cell $\delta S'_{Qrev}$ and the water expelled $\delta S'_{Steam}$, are also in accordance with the literature (Chen; Pei; Song, 2021). As the cell ages, the membrane loses its proton conductivity which increases its internal resistance (Pan et al., 2020), generating heat from Joule effects. A higher water expelling, on the other hand, can generate problems of membrane dehydration decreasing ions movement. Still, these two parameters need a little more attention. Due to the thermodynamics model simplifications and the lack of data regarding PEMFC water management and temperature gradients, these results are mainly related to the cell operation current load, and further investigation are suggested to future works.

It can also be noticed that the magnitude of the gradients for 70A is higher for 3A. This result is in accordance with what is observed in real PEMFC degradation. The higher the current load, the faster the PEMFC loses its ability to generate power (Chen; Pei; Song, 2021). This suggests that the degradation entropy generation combined with the RNN method can predict the degradation not only on a constant specific load but also on different load conditions. As observed, Equation 8 remains the same, being independent from the health indicators, so the neural networks weights act here predicting different degradation trends for different load conditions.

Figure 18 – Degradation Entropy Generation coefficients for 3 and 70A.

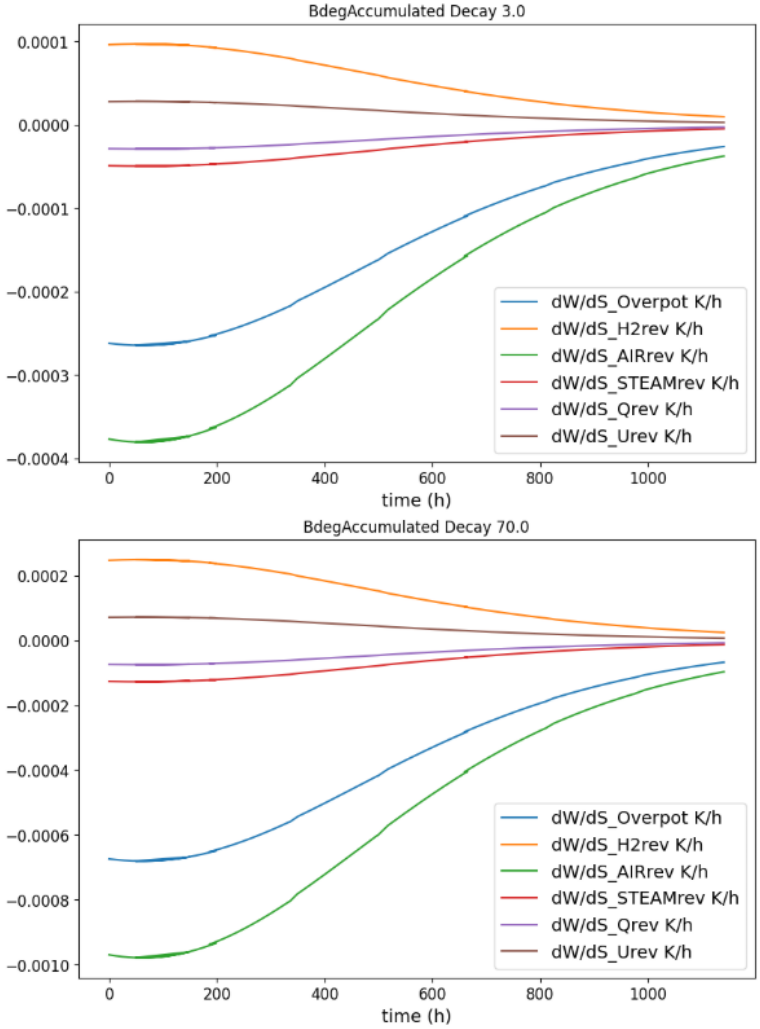

Source: (author production).

Legend: The blue line represents the degradation coefficient related to the cell overpotential, the yellow line represents the coefficient related to the hydrogen transport to the cell, the green line represents the coefficient related to the air transport to the cell, the red line represents the coefficient related to the water expelled by the cell, the purple line represents the coefficient related to the heat exchange and the brown line represents the coefficient related to the internal energy change of the cell.

The RUL predictions using the 70A polarization point decay and the entropy generation due to the overvoltage $S'_{overpot}$ affecting the cell are exhibited at Figure 19

and Figure 20, respectively. The model was able to predict the RUL with significant margin to maintenance procedures for both criteria in the training set and the test set. Still, even using a stricter trusting area, the prognostic horizon is higher for the $S'_{overpot}$ metric, showcasing its importance in long term degradation prediction.

Figure 19 – Prognostic Horizon for 70A decay as health indicator for train (FC1) and test set (FC2)

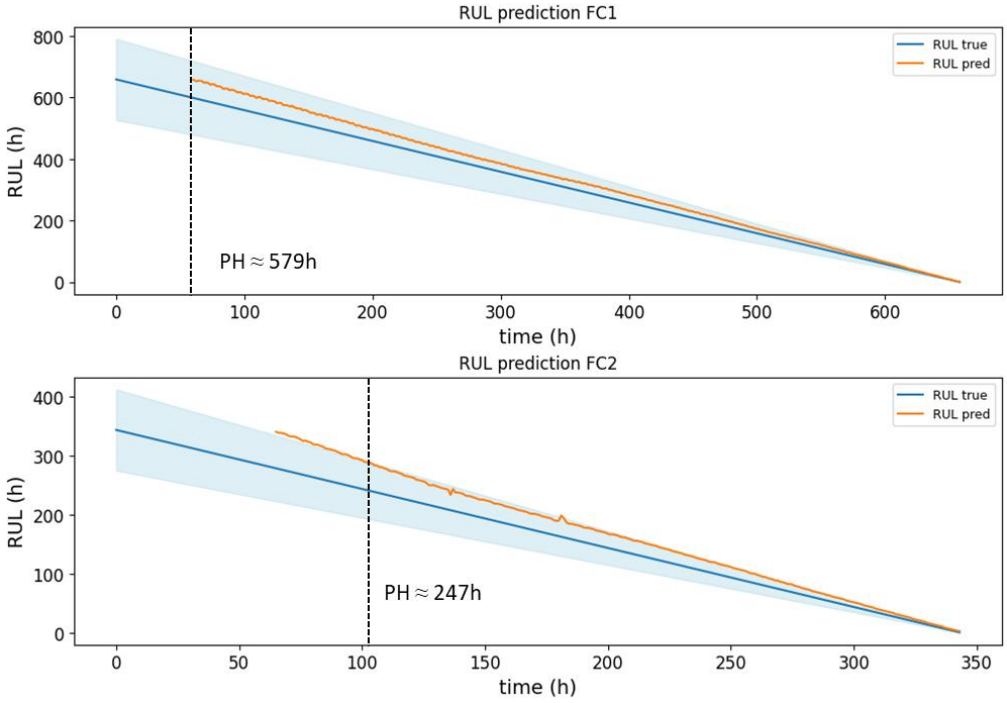

Source: (author production).

Figure 20 – Prognostic Horizon for entropy generation due to PEMFC overvoltage as health indicator for train (FC1) and test set (FC2)

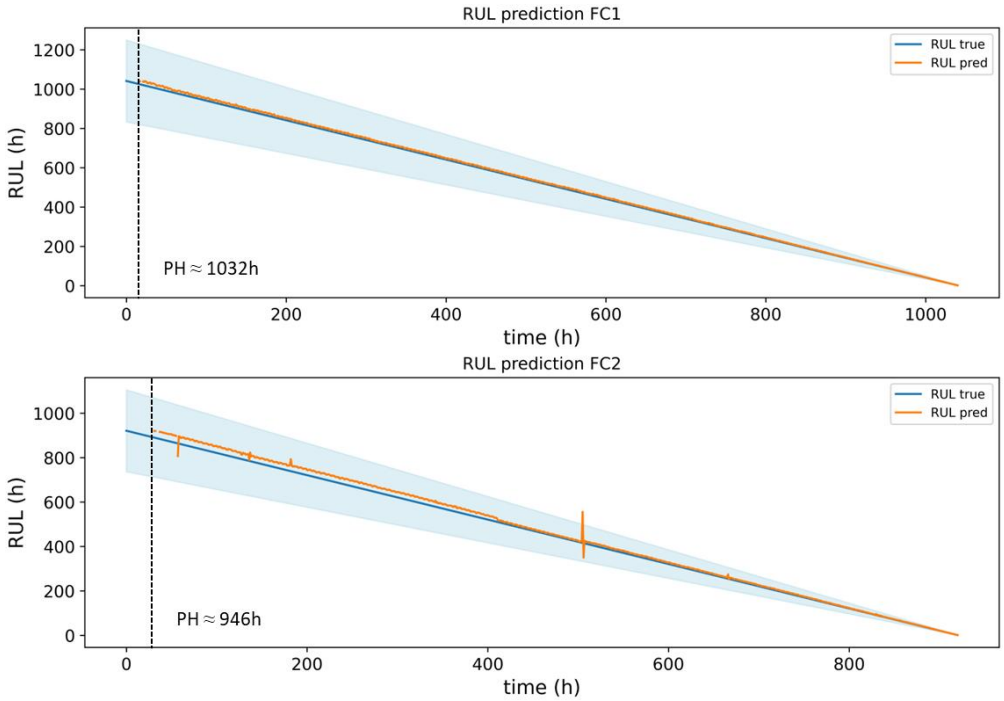

Source: (author production).

The usage of a non-measurable metric of degradation for prognostics is not a new contribution from this work. As mentioned in section 4.6, Bressel et al (Bressel et al., 2016) proposed the usage of α_{degr} to predict the RUL. Still, differently from α_{degr}, the entropy generation due to the cell overvoltages has a real interpretable physical meaning, related to the cell usage, age and voltage losses which makes it more informative and therefore suitable for maintenance procedures.

5 CONCLUSION

Given that PEMFC degradation can be caused by several reasons such as thermal and mechanical stress, humidity, variable load profiles and start/stop conditions; PEMFC prognostics is inherently complex. While data-driven methods lack generalization and interpretability, model-based ones lack accuracy and ease to be applied. Therefore, the present work proposed to develop a hybrid-method, combining the strengths of each methodology in order to predict long-term degradation of PEMFC. The recurrent neural network was used to model the time dependency of the data and propagate current states through time, and the degradation entropy generation theorem was used to train the model when characterization data was not available and provide insights of degradation mechanisms inside the PEMFC. Even though the DEG theorem had already been applied to evaluate degradation in lithium-ion and lead-acid batteries, its application to PEMFC prognostics alongside with physics informed neural networks is a novelty method proposed here.

The proposed model was trained under constant load conditions and able to predict future degradation under semi-dynamic load conditions satisfactorily. Due to its linearity, future entropy generation of the fuel cell was predicted with high accuracy reaching $R^2 = 1$ to all predictions. It was observed that since entropy generation is highly correlated to degradation and is easily predicted, its usage for long term degradation prediction is significant.

The model was also able to predict long term polarization curves decay with high accuracy, reaching a maximum RMSE of 16mV for seen data points and a maximum of 27mV for unseen data points in the test data, showcasing its generalization capability. The polarization decay trend exhibited a linear exponential decay pattern suggesting that eventually the cell would reach a maximum degradation state.

A metric related to gases' consumption efficiency was also proposed to evaluate PEMFC future fuel needs. The hydrogen efficiency was predicted accurately but that was not the case for the oxygen. It was observed that since the train and test set for this metric did not follow the same pattern, the model struggles to be trained

and predict accurate results. It was suggested that faults in water management may be the reason affecting the test set.

Through repeatedly propagating future state predictions and defining an end-of-life criteria the remaining useful life of the cell was obtained. It was observed that in the absence of a better metric to evaluate the EOL, the entropy generation due to the cell overvoltage could be used. Due to the strong relationship between this metric and degradation and the ease to predict it, entropy generation could be of great use to long term degradation estimations giving higher prognostic horizons to maintenance procedures.

Future work is suggested to improve the hybrid model limitations. The main limitation that should be addressed is the lack of dynamic data, that better represents real operating conditions of fuel cells to test the model. In addition, other limitations that should be addressed arise from the simplifications used to obtain the thermodynamic model such as the assumption that all the water that enters and is produced by the PEMFC control volume is expelled. As observed, a model-based method relating water contents and gases consumption efficiency would benefit the hybrid-model greatly.

REFERENCES

AO, Y. *et al*. Proton exchange membrane fuel cell prognosis based on frequency-domain Kalman filter. **IEEE Transactions on Transportation Electrification**, New York, 2021.

BARBIR, F. **PEM fuel cells**: theory and practice. 2. ed. Waltham: Academic Press, 2012. 518 p.

BAR-ON, I.; KIRCHAIN, R.; ROTH, R. Technical cost analysis for PEM fuel cells. **Journal of Power Sources**, Lausanne, v. 109, n. 1, p. 71-75, 15 jun. 2002.

BRESSEL, M. *et al*. Extended Kalman filter for prognostic of proton exchange membrane fuel cell. **Applied Energy**, London, v. 164, p. 220-227, 15 fev. 2016.

BRUNETTO, C.; MOSCHETTO, A.; TINA, G. PEM fuel cell testing by electrochemical impedance spectroscopy. **Electric Power Systems Research**, Lausanne, v. 79, n. 1, p. 17-26, 1 jan. 2009.

BRYANT, M. D.; KHONSARI, M. M.; LING, F. F. On the thermodynamics of degradation. **Proceedings of the Royal Society A: Mathematical, Physical and Engineering Sciences**, London, v. 464, n. 2096, p. 2001-2014, 1 ago. 2008.

CASTELINO, P. *et al*. Degradation mechanisms in PEM fuel cells: a brief review. **Materials Today: Proceedings**, Amsterdam, v. 35, p. 412-416, 3 abr. 2023.

CHEN, H. *et al*. Whole life cycle performance degradation test and RUL prediction research of fuel cell MEA. **Applied Energy**, London, v. 310, p. 118556, 15 mar. 2022.

CHEN, H.; PEI, P.; SONG, M. Thermodynamic and economic study of PEMFC stack considering degradation characteristic. **Energy Conversion and Management**, Oxford, v. 235, p. 114016, 1 maio 2021.

DOELLING, K. L. *et al*. An experimental study of the correlation between wear and entropy flow in machinery components. **Journal of Applied Physics**, Melville, v. 88, n. 5, p. 2999-3003, 1 set. 2000.

HUA, Z. *et al*. Remaining useful life prediction of PEMFC systems based on the multi-input echo state network. **Applied Energy**, London, v. 272, p. 115250, 15 ago. 2020.

HUA, Z. *et al*. A review on lifetime prediction of proton exchange membrane fuel cells system. **Journal of Power Sources**, Lausanne, v. 529, p. 231256, 1 maio 2022.

JAVED, K. *et al*. Prognostics of Proton Exchange Membrane Fuel Cells stack using an ensemble of constraints based connectionist networks. **Journal of Power Sources**, Lausanne, v. 324, p. 745-757, 30 ago. 2016.

JIN, J. *et al*. Degradation prediction of PEMFC based on data-driven method with adaptive fuzzy sampling. **IEEE Transactions on Transportation Electrification**, Piscataway, v. 10, n. 2, p. 3363-3372, jun. 2024.

JOUIN, M. *et al*. Prognostics of PEM fuel cell in a particle filtering framework. **International Journal of Hydrogen Energy**, Oxford, v. 39, n. 1, p. 481-494, 2 jan. 2014.

JOUIN, M. *et al*. Prognostics and health management of PEMFC – state of the art and remaining challenges. **International Journal of Hydrogen Energy**, Oxford, v. 38, n. 35, p. 15307-15317, 22 nov. 2013.

KIMOTHO, J. K.; MEYER, T.; SEXTRO, W. PEM fuel cell prognostics using particle filter with model parameter adaptation. *In*: INTERNATIONAL CONFERENCE ON PROGNOSTICS AND HEALTH MANAGEMENT, 2014, Eastern Washington. **Proceedings** [...]. Piscataway: IEEE, 2014. p. 1-6.

KIRUBAKARAN, A.; JAIN, S.; NEMA, R. K. A review on fuel cell technologies and power electronic interface. **Renewable and Sustainable Energy Reviews**, Oxford, v. 13, n. 9, p. 2430-2440, 1 dez. 2009.

KONDEPUDI, D.; PRIGOGINE, I. **Modern thermodynamics**: from heat engines to dissipative structures. 2. ed. Chichester: John Wiley & Sons, 2014.

LI, H. *et al*. A fusion intelligent degradation interval prediction method based on hybrid health indicator for proton exchange membrane fuel cells. **IEEE Transactions on Transportation Electrification**, Piscataway, v. 10, n. 4, p. 9839-9851, dez. 2024.

LI, R.; VERHAGEN, W. J. C.; CURRAN, R. A systematic methodology for Prognostic and Health Management system architecture definition. **Reliability Engineering & System Safety**, Amsterdam, v. 193, p. 106598, 1 jan. 2020.

LIJESH, K. P.; KHONSARI, M. M. Characterization of multiple wear mechanisms through entropy. **Tribology International**, Oxford, v. 152, p. 106548, dez. 2020.

LITSTER, S.; MCLEAN, G. PEM fuel cell electrodes. **Journal of Power Sources**, Lausanne, v. 130, n. 1-2, p. 61-76, 3 maio 2004.

LIU, H. *et al*. Data-based short-term prognostics for proton exchange membrane fuel cells. **International Journal of Hydrogen Energy**, Oxford, v. 42, n. 32, p. 20791-20808, 10 ago. 2017.

LIU, H. *et al*. Prognostics methods and degradation indexes of proton exchange membrane fuel cells: A review. **Renewable and Sustainable Energy Reviews**, Oxford, v. 123, p. 109721, 1 maio 2020.

LIU, X. *et al*. Degradation prediction of fuel cell systems based on different operating conditions in dynamic cycling condition. **Heliyon**, London, v. 10, n. 4, e26057, 29 fev. 2024.

LUCIA, U. Overview on fuel cells. **Renewable and Sustainable Energy Reviews**, Oxford, v. 30, p. 164-169, 1 fev. 2014.

MA, R. *et al*. Data-driven proton exchange membrane fuel cell degradation predication through deep learning method. **Applied Energy**, Oxford, v. 231, p. 102-115, 1 dez. 2018.

MA, R. *et al*. A hybrid prognostic method for PEMFC with aging parameter prediction. **IEEE Transactions on Transportation Electrification**, Piscataway, v. 7, n. 4, p. 2318-2331, dez. 2021.

MORANDO, S. *et al*. Proton exchange membrane fuel cell ageing forecasting algorithm based on Echo State Network. **International Journal of Hydrogen Energy**, Oxford, v. 42, n. 2, p. 1472-1480, 12 jan. 2017.

O'HAYRE, R. *et al*. **Fuel cell fundamentals**. 3. ed. Hoboken: John Wiley & Sons, 2016.

OSARA, J. A.; BRYANT, M. D. A thermodynamic model for lithium-ion battery degradation: application of the degradation-entropy generation theorem. **Inventions**, Basel, v. 4, n. 2, art. 23, p. 1-21, 3 abr. 2019a.

OSARA, J. A.; BRYANT, M. D. Thermodynamics of fatigue: degradation-entropy generation methodology for system and process characterization and failure analysis. **Entropy**, Basel, v. 21, n. 7, art. 685, p. 1-25, 12 jul. 2019b.

OSARA, J. A.; BRYANT, M. D. Thermodynamics of grease degradation. **Tribology International**, Oxford, v. 137, p. 433-445, 1 set. 2019c.

OSARA, J. A.; BRYANT, M. D. Thermodynamics of lead-acid battery degradation: application of the degradation-entropy generation methodology. **Journal of The Electrochemical Society**, Pennington, v. 166, n. 16, p. A4188-A4203, 19 dez. 2019d.

OSARA, J. A.; BRYANT, M. D. Methods to calculate entropy generation. **Entropy**, Basel, v. 26, n. 3, art. 237, p. 1-21, 7 mar. 2024.

PAN, R. *et al*. Health degradation assessment of proton exchange membrane fuel cell based on an analytical equivalent circuit model. **Energy**, Oxford, v. 207, e118185, p. 1-11, 15 set. 2020.

PENG, W. *et al*. A hybrid health prognostics method for proton exchange membrane fuel cells with internal health recovery. **IEEE Transactions on Transportation Electrification**, Piscataway, v. 10, n. 2, p. 3062-3072, jun. 2024.

PETRONE, R. *et al*. A review on model-based diagnosis methodologies for PEMFCs. **International Journal of Hydrogen Energy**, Oxford, v. 38, n. 17, p. 7077-7091, 10 jun. 2013.

POLVERINO, P.; PIANESE, C. Model-based prognostic algorithm for online RUL estimation of PEMFCs. *In*: CONFERENCE ON CONTROL AND FAULT-TOLERANT SYSTEMS, SYSTOL, 3., 2016, Barcelona. **Proceedings** [...]. Piscataway: IEEE, 2016. p. 599-604.

QURESHY, A. M. M. I.; DINCER, I. Modeling-based analytics of degradation behavior for fuel cell stack under actual dynamic ambient temperature. **Energy Conversion and Management**, Oxford, v. 269, e116100, p. 1-16, 1 out. 2022.

RAISSI, M.; PERDIKARIS, P.; KARNIADAKIS, G. E. Physics-informed neural networks: a deep learning framework for solving forward and inverse problems involving nonlinear partial differential equations. **Journal of Computational Physics**, San Diego, v. 378, p. 686-707, 1 fev. 2019.

RAMOUSSE, J. *et al*. Modelling of heat, mass and charge transfer in a PEMFC single cell. **Journal of Power Sources**, Amsterdam, v. 145, n. 2, p. 416–427, 18 ago. 2005.

RANALLI, J. *et al*. An online tool for facilitating thermodynamic property lookups. *In*: ASEE ANNUAL CONFERENCE & EXPOSITION, 129., 2022, Minneapolis. **Proceedings** [...]. Washington, DC: ASEE, 2022.

SHAH, R. K. Introduction to fuel cells. *In*: BASU, S. (ed.). **Recent trends in fuel cell science and technology**. New Delhi: Anamaya Publishers; New York: Springer, 2007. p. 1-9.

SHARAF, O. Z.; ORHAN, M. F. An overview of fuel cell technology: fundamentals and applications. **Renewable and Sustainable Energy Reviews**, Oxford, v. 32, p. 810-853, 1 abr. 2014.

SILVA, R. E. *et al*. Proton exchange membrane fuel cell degradation prediction based on Adaptive Neuro-Fuzzy Inference Systems. **International Journal of Hydrogen Energy**, Oxford, v. 39, n. 21, p. 11128-11144, 15 jul. 2014.

SUTHARSSAN, T. *et al*. Prognostic and health management for engineering systems: a review of the data-driven approach and algorithms. **The Journal of Engineering**, Stevenage, v. 2015, n. 7, p. 215-222, jul. 2015.

SUTHARSSAN, T. *et al*. A review on prognostics and health monitoring of proton exchange membrane fuel cell. **Renewable and Sustainable Energy Reviews**, Oxford, v. 75, p. 440-450, 1 ago. 2017.

TANER, T. Alternative energy of the future: a technical note of PEM fuel cell water management. **Journal of Fundamentals of Renewable Energy and Applications**, Los Angeles, v. 5, n. 3, art. 1000163, p. 1-3, 2015. Disponível em: https://www.researchgate.net/publication/283259049_Alternative_Energy_of_the_Future_A_Technical_Note_of_PEM_Fuel_Cell_Water_Management. Acesso em: 23 set. 2025.

THE, L. H. ISO standards for condition monitoring. *In*: ENGINEERING ASSET MANAGEMENT: PROCEEDINGS OF THE 1ST WORLD CONGRESS ON ENGINEERING ASSET MANAGEMENT (WCEAM), 1., 2006, Gold Coast. **Proceedings** [...]. London: Springer, 2006. p. 606–613.

TIAN, Q. *et al*. Remaining useful life prediction method of PEM fuel cells based on a hybrid model. **Electronics**, Basel, v. 12, n. 1, art. 7, p. 1–17, 2023.

UNIVERSITÉ DE FRANCHE-COMTÉ. FEMTO-ST Institute. **dat@UBFC**: IEEE PHM Data Challenge 2014. Besançon: UBFC, 2021. Disponível em: https://search-data.ubfc.fr/FR-18008901306731-2021-07-19_IEEE-PHM-Data-Challenge-2014.html. Acesso em: 23 set. 2025.

VICHARD, L. *et al*. Degradation prediction of PEM fuel cell based on artificial intelligence. **International Journal of Hydrogen Energy**, Oxford, v. 45, n. 29, p. 14953-14963, 29 maio 2020.

VIRTANEN, P. *et al*. **scipy/scipy**: SciPy 1.16.2. Versão 1.16.2. Zenodo, 11 set. 2025. 1 recurso eletrônico.

WANG, C. *et al*. Data-driven prognostics based on time-frequency analysis and symbolic recurrent neural network for fuel cells under dynamic load. **Reliability Engineering & System Safety**, Amsterdam, v. 231, art. 108990, p. 1-12, mar. 2023.

WANG, P. *et al*. A novel degradation model of proton exchange membrane fuel cells for state of health estimation and prognostics. **International Journal of Hydrogen Energy**, Oxford, v. 46, n. 60, p. 30829-30839, 27 ago. 2021.

WANG, T.; ZHOU, H.; ZHU, C. A short-term and long-term prognostic method for PEM fuel cells based on Gaussian process regression. **Energies**, Basel, v. 15, n. 21, art. 8234, p. 1-17, 2022.

WU, H. *et al*. Hybrid physics-based and data-driven prognostic for PEM fuel cells considering voltage recovery. **IEEE Transactions on Energy Conversion**, Piscataway, v. 39, n. 2, p. 1120-1131, jun. 2024.

XU, J.-H. *et al*. Multi-criteria evaluation and optimization of PEM fuel cell degradation system. **Applied Energy**, Oxford, v. 332, art. 120485, p. 1-15, 15 fev. 2023.

YANG, Y. *et al*. Degradation prediction of proton exchange membrane fuel cells with model uncertainty quantification. **Renewable Energy**, Oxford, v. 219, pt. 2, art. 119525, p. 1-13, dez. 2023.

YU, Y. *et al*. Deep learning with dual-stage attention mechanism for interpretable prediction of proton exchange membrane fuel cell performance degradation. **International Journal of Hydrogen Energy**, Oxford, v. 51, pt. B, p. 1162-1173, 11 jan. 2024a.

YU, Y. *et al*. Degradation and polarization curve prediction of proton exchange membrane fuel cells: an interpretable model perspective. **Applied Energy**, Oxford, v. 353, pt. A, art. 122081, p. 1-13, 1 jan. 2024b.

YUE, M. *et al*. Proton exchange membrane fuel cell system prognostics and decision-making: current status and perspectives. **Renewable Energy**, Oxford, v. 179, p. 2277-2294, 1 dez. 2021.

ZHANG, C. *et al*. A comparative study of using polarization curve models in proton exchange membrane fuel cell degradation analysis. **Energies**, Basel, v. 13, n. 15, art. 3759, p. 1-20, 22 jul. 2020.

ZHANG, X.; PISU, P. Prognostic-oriented fuel cell catalyst aging modeling and its application to health-monitoring and prognostics of a PEM fuel cell. **International Journal of Prognostics and Health Management**, Rochester, v. 5, n. 1, art. 004, p. 1-13, 2014.

ZHOU, J. *et al*. A real-time prediction method for PEMFC life under actual operating conditions. **Sustainable Energy Technologies and Assessments**, Amsterdam, v. 65, art. 103770, p. 1-13, maio 2024.

APENDIX A – PEMFC ENTROPY GENERATION MODEL

Through the local equilibrium hypothesis, the first and second laws of thermodynamics were applied to the PEMFC stack control volume, according to Equation 23 and 24 (Kondepudi; Kitchin, 2014):

$$dU = \delta Q - pdV + \sum h_e dN_e + \sum \tilde{\mu}_k dN_k \tag{23}$$

$$dS = dS_{irr} = \frac{\delta Q}{T} + \sum \frac{h_e dN_e}{T} + \delta S' \tag{24}$$

In which dU represents the internal energy variation of the control volume; δQ is the heat exchange with the environment; pdV is the mechanical work performed; which for the case of the cell is zero (only electrical work is performed); $h_e dN_e$ is the enthalpy variation of the element e that passes through the control volume; $\tilde{\mu}_k dN_k$ is the variation of the electrochemical potential of the element k within the control volume; dS is the variation of entropy; and $\delta S'$ is the generation of entropy. Replacing 24 in 23 we get Equation 25:

$$T\delta S' + dU = TdS + \sum \mu_k dN_k = T\delta S_{U,phen} \tag{25}$$

in which $\delta S_{U,phen}$ is the change of entropy through the phenomenological path, evaluated through Equation 25. Here, differently from what was proposed for batteries in (Osara; Bryant, 2019a) and in Equation 6, we are evaluating the change of entropy in terms of internal energy change $\delta S' = \delta S_{U,phen} - dS_{U,rev}$. Solving for $\delta S'$, we get Equation 26:

$$\delta S' = dS - \frac{\delta W}{T} + \sum \frac{\mu_k dN_k}{T} - \frac{dU}{T} \tag{26}$$

Considering that the difference between two thermodynamic states is independent on the process path, then $dS = dS_{irr} = dS_{rev}$. In this way, dS is defined by Equation 27.

$$dS = dS_{rev} = \frac{\delta Q_{rev}}{T} + \sum \frac{h_{rev} dN_e}{T} \tag{27}$$

For the reversible path, the states of the gases entering and leaving the cell will be considered equal $\left(h_{e,inlet} = h_{e,exit}\right)$, therefore we will use $h_{e,exit}$ to reflect a fuel cell operating reversibly with a pressure smaller than expected, which correlates better with a degradation analysis. In Equation (28), we also replace $dN_e = \frac{dm_e}{MM_e}$, in which dm_e is the mass change of substance e in the control volume and MM_e is its molar mass.

$$\delta S' = \frac{\delta Q_{rev}}{T} + \sum \frac{h_{e,exit} dm_e}{T MM_e} + \sum \frac{\tilde{\mu}_k dN_k}{T} - \frac{dU}{T} \tag{28}$$

Invoking again that the difference between two states is independent on the process path, then $dU = dU_{irr} = dU_{rev}$. From (Osara; Bryant, 2024), we get that for a boundary loaded system, the reversible change in its internal energy equals the maximum work possible. For the PEMFC, it is the maximum energy available from its fuel (Equation 29):

$$\frac{dU_{rev}}{T} = \frac{LHV_{H2} dm_{H2}}{T} \tag{29}$$

in which LHV_{H2} is the lower heating value of the fuel (hydrogen gas) and dm_{H2} is the fuel consumption. We are using the lower heating value of the fuel because we are considering here that water only leaves the system as vapor. From (Ramousse et al., 2005), we get that heat is generated and absorbed in the cell through the following mechanisms:

1. Ionic resistivity of polymer membrane
2. Electrochemical reactions on the electrodes
3. Overvoltages at the electrodes
4. Absorption or elimination of water in the membrane

Out of the four of them, only mechanisms 2 and 4 can generate or consume heat (depending on the direction of the reaction and if the system is absorbing or eliminating water), and therefore can be viewed as reversible heat transfer. Considering here that all water produced by the cell leaves the system, the reversible heat transfer equals the heat produced by the reactions:

$$\delta Q_{reac} = h_{reac} d\xi = \left[h_{o,f}^{H2O} + \left(c_p^{H2O}(T) - \frac{1}{2} c_p^{O2}(T) - c_p^{H2}(T) \right) dT \right] d\xi \quad (30)$$

In Equation 30, h_{reac} is the molar enthalpy of the reaction; $d\xi$ is the extent of the reaction (number of times the oxidation-reduction reaction has happened); $h_{o,f}^{H2O}$ is the enthalpy of formation of water at standard state; and c_p^k the heat capacity of substance k at constant pressure. Here, we are assuming that the reaction at the anode and at the cathode are coupled ($d\xi_{ano} = d\xi_{cat} = d\xi$), resulting in Equation 31.

$$\delta S' = \frac{h_{reac} d\xi}{T} + \sum \frac{h_{e,exit} dm_e}{T M M_e} + \sum \frac{\tilde{\mu}_k dN_k}{T} - \frac{LHV_{H2} dm_{H2}}{T} \quad (31)$$

Now, replacing in Equation 31 the change in moles dN_k of substance k for the change in the extent of reaction times the stoichiometric factor υ_k of each reactant ($dN_k = \upsilon_k d\xi$) and recalling the definition of electrochemical potentials $\tilde{\mu}_k = \mu_k + zF\phi_k$, we get the electrochemical energy change of the cell (Equation 32):

$$\tilde{A} d\xi = \left[2(\mu_{cat}^{H+} - \mu_{ano}^{H+}) + 2(\mu_{cat}^{e-} - \mu_{ano}^{e-}) + (\mu_{ano}^{H2} + \frac{1}{2}\mu_{cat}^{O2} - \mu_{cat}^{H2O}) + 2F(\phi_{ano} - \phi_{cat}) \right] d\xi \quad (32)$$

Here, $\tilde{A} = \sum \upsilon_k \tilde{\mu}_k$ is Donder's electrochemical affinity; μ^i is the chemical potential of reactant i; F is Faraday's constant; and ϕ_z are the electric potential of the electrode z. By using the definition of the chemical potentials $\mu^i = \mu_0^i + RT \ln(a^i)$, in which μ_0^i is the chemical potential at standard state; R is the ideal gas constant; and a^i is the activity of i and recalling that for electrons in metals $a_{metals}^{e-} = 1$, the second term on the right side of Equation 32 vanishes, resulting in Equation 33:

$$\tilde{A} d\xi = \left[2(\mu_{cat}^{H+} - \mu_{ano}^{H+}) + (\mu_{ano}^{H2} + \frac{1}{2}\mu_{cat}^{O2} - \mu_{cat}^{H2O}) + 2F(\phi_{ano} - \phi_{cat}) \right] d\xi \quad (33)$$

Since for the PEMFC, the transport of H^+ ions is mostly due to conduction than it is due to diffusion, i.e. $\Delta\phi_{\frac{ano}{cat}} \gg \Delta\mu_{\frac{ano}{cat}}^{H+}$, we can neglect the first term on the right side of Equation 33 (O'hayre et al., 2016), resulting in Equation (34):

$$\tilde{A}d\xi = \left[\left(\mu_{0,ano}^{H2} + \frac{1}{2}\mu_{0,cat}^{O2} - \mu_{0,cat}^{H2O}\right) + RTln\left(\frac{a_{ano}^{H2}(a_{cat}^{O2})^{\frac{1}{2}}}{a_{cat}^{H2O}}\right) + 2F(\phi_{ano} - \phi_{cat})\right]d\xi \quad (34)$$

In Equation 34, since the difference in electric potential between the two electrodes represents the voltage output by the cell $\phi_{ano} - \phi_{cat} = -V$ (Kondepudi; Kitchin, 2014) (by convention, the reduction potential is considered positive) and the change in the extent of reaction dξ can be easily obtained by the change in mols of electrons $d\xi = dq/2F$, the last term on the right side of the equation is simply the electric work performed by the cell $(-Vdq)$, as shown in Equation 35.

$$\tilde{A}d\xi = \left[\left(\mu_{0,ano}^{H2} + \frac{1}{2}\mu_{0,cat}^{O2} - \mu_{0,cat}^{H2O}\right) + RTln\left(\frac{a_{ano}^{H2}(a_{cat}^{O2})^{\frac{1}{2}}}{a_{cat}^{H2O}}\right)\right]\frac{dq}{2F} - Vdq \quad (35)$$

If the cell is in equilibrium at standard state, $\tilde{A}d\xi = 0$ and $\mu^i = \mu_0^i$ (Equation(36)):

$$E = \left[\left(\mu_{0,ano}^{H2} + \frac{1}{2}\mu_{0,cat}^{O2} - \mu_{0,cat}^{H2O}\right)\right]\frac{1}{2F} \quad (36)$$

In which E is the cell's electromotive force. For a single cell, $E \approx 1.23\,V$. Substituting Equation 36 in Equation 35, we get Equation 37:

$$\tilde{A}d\xi = \left[E - V + \frac{RT}{2F}ln\left(\frac{a_{ano}^{H2}(a_{cat}^{O2})^{\frac{1}{2}}}{a_{cat}^{H2O}}\right)\right]dq \quad (37)$$

From the literature (O'hayre et al., 2016), we know that the sum of the first and the third terms on the right side of Equation 37 are the Nernst voltage of the cell, i.e. $E_{corr} = E - \frac{RT}{nF}\ln\left(\frac{a_{prods}}{a_{reacts}}\right)$. Therefore:

$$\tilde{A}d\xi = [E_{corr} - V]dq = \eta dq \quad (38)$$

in which η is the cell overvoltage. Replacing Equation 38 in Equation 28, we get Equation 39.

$$\delta S' = \frac{h_{reac} dq}{2TF} + \sum \frac{h_{e,exit} dm_e}{TMM_e} + \frac{\eta dq}{T} - \frac{LHV_{H2} dm_{H2}}{T} \quad (39)$$

From [57], we know that the PEMFC overpotential η manifests itself in three forms:

Activation Overvoltages η_{act} , which account for reaction kinetics losses at electrode/electrolyte interfaces. In this work we will consider only the cathode's activation loss, since the oxygen reduction reaction is much slower than the hydrogen oxidation reaction (Pan et al., 2020). It can be modeled using Tafel's equation:

$$\eta_{act} = \frac{RT}{\alpha nF} ln(i) - \frac{RT}{\alpha nF} ln(i_o) \quad (40)$$

in which i is the current load; i_o is the equilibrium exchange current; and α the symmetry factor of the reaction.

Ohmic Overvoltages η_{ohm}, which account for the transport of H^+ losses at the electrolyte and obey Ohm's law:

$$\eta_{ohm} = R_{ohm} i \quad (41)$$

in which R_{ohm} is the electrolyte's resistance to the passage of charges.

Concentration Overvoltages η_{conc} , which account for reactants concentration losses at electrodes:

$$\eta_{conc} = \frac{RT}{nF}\left(1 + \frac{1}{\alpha}\right) ln\left(\frac{i_l}{i_l - i}\right) \quad (42)$$

In Equation 42, i_l is the limiting current of the cell, which can be evaluated through Equation 43:

$$i_l = \frac{nFAD_{O2,cat} c_{O2}^{bulk}}{\delta_{cat}} \quad (43)$$

Here, A is the electrode's area; $D_{O2,cat}$ is diffusion coefficient of oxygen in the electrode; c_{O2}^{bulk} is the oxygen concentration at the bulk; and δ_{cat} is the cathode

thickness (we are assuming that the diffusive layer thickness equals the cathode thickness).

The overall overpotential is:

$$\eta = \eta_{act} + \eta_{ohmic} + \eta_{conc} \tag{44}$$

Replacing Equation 44 in Equation 39 we get the final entropy generation model of the PEMFC (Equation 45). The entropy generation $\delta S'$, and therefore, the degradation dw is a function of: the temperature of the cell T; the load profile dq; gases consumption dm_e; states $h_{e,exit}$ and activity a_e; electrolyte's resistance R_{ohm}; equilibrium exchange current i_o; symmetry factor of the reaction α; and the limiting current i_l.

$$\delta S' = \frac{h_{reac} dq}{2TF} + \sum \frac{h_{e,exit} dm_e}{TMM_e} + \frac{(\eta_{act} + \eta_{ohmic} + \eta_{conc}) dq}{T} - \frac{LHV_{H2} dm_{H2}}{T} \tag{45}$$

The first five parameters $\left(T , dq , dm_e, h_{e,exit}, a_e \right)$ are external parameters that can be easily measured in day-to-day use of the PEMFC. The other parameters $(R_{ohm}, i_o, \alpha, i_l)$ are internal parameters that directly impact the output power of the cell and can be measured through characterization methods only, which usually are performed at fixed time intervals.

DADOS CURRICULARES

IDENTIFICAÇÃO	
	JOÃO PEDRO RIBEIRO ROSA 11/10/2000
Nacionalidade	brasileira
Nome em citações bibliográficas:	Rosa, João Pedro Ribeiro Rosa, J. P. R. R.
Currículo Lattes	URL http://lattes.cnpq.br/2903294493203822
ORCID	URL https://orcid.org/0009-0002-1253-8580
FORMAÇÃO ACADÊMICA	
2018/2023	Engenheiro Mecânico pela UNESP, Faculdade de Engenharia e Ciências de Guaratinguetá
PRODUÇÃO BIBLIOGRÁFICA	
ROSA, J. P. R. ; MATELLI, J. A. ; SILVA, F. S. . Resilience evaluation of cogeneration systems for hospitals. In: ENCIT 2024 - 20th Brazilian Congress of Thermal Sciences and Engineering, 2024, Foz do Iguaçu. Proceeding of the ENCIT 2024, 2024.	
PARTICIPAÇÃO EM BANCAS E ORIENTAÇÕES	
Bancas de trabalhos de conclusão	
Não houveram participações em bancas.	
Orientações	
Não houveram orientações.	
PARTICIPAÇÃO EM EVENTOS CIENTÍFICOS	
ENCIT 2024 - 20th Brazilian Congress of Thermal Sciences and Engineering, 2024, Foz do Iguaçu. Resilience evaluation of cogeneration systems for hospitals. 2024.	